THE ASTROPHYSICAL JOURNAL, 443:735–752, 1995 April 20

TEMPERATURES, GRAVITIES, AND MASSES FOR A SAMPLE OF BRIGHT DA WHITE DWARFS AND THE INITIAL-TO-FINAL MASS RELATION[1]

ANGELA BRAGAGLIA
Osservatorio Astronomico di Bologna, CP 596, I-40126 Bologna, Italy;
angela@astbo3.bo.astro.it

ALVIO RENZINI
Dipartimento Astronomia, Università di Bologna, CP 596, I-40126 Bologna, Italy;
alvio@astbo3.bo.astro.it

AND

P. BERGERON
Département de Physique, Université de Montréal, C.P. 6128, Succ. Centre-Ville, Montréal, Québec, Canada H3C 3J7;
bergeron@astro.umontreal.ca
Received 1994 July 11; accepted 1994 October 27

ABSTRACT

The atmospheric parameters, $T_{\rm eff}$ and log g, have been determined for a sample of 52 hydrogen-line (DA) white dwarfs by fitting optical spectra to theoretical model atmospheres. Multiple observations of each star allow an estimation of the accuracy of the method: the average external errors are 490 K in $T_{\rm eff}$ and 0.06 in log g.

Masses have been derived using white dwarf evolutionary models where finite temperature effects are taken into account. The average mass of the 46 DA stars in our sample with $T_{\rm eff} > 12{,}000$ K is 0.587 $M_\odot$, with a dispersion of 0.166 $M_\odot$ while the mode of the distribution is between 0.50 and 0.55 $M_\odot$. The mass distribution shows a low-mass ($M < 0.4\ M_\odot$) tail of four objects which are most likely helium white dwarfs, the outcome of close binary evolution. Excluding those objects, the average mass becomes 0.609 $M_\odot$, with a dispersion of 0.157 $M_\odot$. When combining with the sample studied by Bergeron, Saffer, & Liebert (1992), this leads to a set of 164 white dwarfs for which atmospheric parameters and masses have been obtained in a homogeneous way. In this sample 15 objects have $M < 0.4\ M_\odot$, thus confirming that about 10% of catalog white dwarfs are helium white dwarfs produced in close binaries. The implications for the stellar initial mass-final mass relation are then discussed in some detail. Some individual objects of particular astrophysical interest are also briefly discussed.

Subject headings: stars: evolution — stars: fundamental parameters — stars: luminosity function, mass function — white dwarfs

1. INTRODUCTION

White dwarfs (WD) are the evolutionary end-product of most stars, either single or in binary systems. Their study can thus provide unique information for our understanding of crucial aspects of the whole previous evolution. In particular, from the WD mass distribution one can infer constraints on the initial mass-final mass relation (IMFMR), and therefore on the total amount of mass that each star loses in the course of its entire evolution. In turn, the IMFMR is an essential ingredient in evaluating the evolution of the mass budget of stellar populations and galaxies (e.g., Renzini & Buzzoni 1986). In the case of WDs in binaries, a knowledge of their mass will shed additional light on the total amount of mass and angular momentum lost by the system in the course of one or more common envelope events. WDs are also important tools for investigating the history of the Galaxy, and in particular, to estimate the age of the local disk (Winget et al. 1987; Iben & Laughlin 1989; Wood 1992). For all the reasons above, the accurate determination of the mass of individual WDs is therefore of great interest. These and other aspects of WD astrophysics have been thoroughly reviewed by Weidemann (1990).

Temperatures, surface gravities, and masses of white dwarf stars have been determined in several dedicated studies (e.g., Koester, Schulz, & Weidemann 1979, hereafter KSW; Shipman 1979; Weidemann & Koester 1984; McMahan 1989; Kidder 1991; Bergeron, Saffer, & Liebert 1992, hereafter BSL). A critical review of these earlier analyses (except that of Kidder 1991) is presented at length in BSL.

Using high signal-to-noise (S/N) CCD spectra of relatively bright WDs, BSL were able to determine temperatures and surface gravities of improved accuracy for 129 WDs of the DA variety, using Balmer line fitting to model atmospheres. WD masses were then derived from the evolutionary models of Wood (1990). In the present paper we expand their study by applying the same procedure to a sample of 52 DA stars (hereafter referred to as the "ESO sample"), 11 of which are in common with the sample of BSL. The original motivation for the collection of all the data used in this work was a CCD spectroscopic survey aimed at discovering the so-called double degenerate (DD) systems (Bragaglia et al. 1990, hereafter BGRD), i.e., binary systems formed by two WDs. Such systems have been proposed as possible progenitors of Type Ia supernovae (Iben & Tutukov 1984; Webbink 1984; Paczyński 1985), an aspect whose developments are discussed elsewhere (Bragaglia, Greggio, & Renzini 1995; Renzini 1993).

This paper is organized as follows. In § 2 the observations and data reduction are described. The data analysis and the

[1] Based on observations obtained at ESO telescopes, La Silla, Chile.

derived WD parameters are presented in § 3. A star-by-star comparison with previous WD parameter determinations is presented in § 4. The resulting WD mass distribution for the present sample, as well as the one combined with the BSL sample, is presented in § 5. Objects of particular astrophysical interest are briefly discussed in § 6. In § 7 the empirical WD mass distribution is discussed in the context of theoretical expectations, and inferences concerning the IMFMR are derived.

2. OBSERVATIONS AND REDUCTIONS

2.1. *The Sample*

The objects discussed in this paper are part of a large sample of bright field WDs that were inspected for binarity, chosen (as a rule) from the "Catalog of Spectroscopically Identified White Dwarfs" (McCook & Sion 1987) and observed at the ESO telescopes. Selection criteria for the objects were fairly simple: they had to be bright enough as to ensure short exposure times (i.e., better time resolution in the binary search for short-period systems), they should not have any known peculiarity such as unusually high magnetic fields, and, possibility, they should be quite hot, hence young (to ensure that an eventual binary motion would show up in line position shifts and not in line profile variations, since the first are better measured by the cross-correlation technique used). Seven objects in the sample of 54 WD candidates presented by BGRD turned out to be hot subdwarfs and two were composite DA + Red Dwarf systems. The subdwarfs were identified from the presence of helium lines in addition to the dominant Balmer lines (only He I for the sdB's, and He I plus He II for the sdO's). At the low resolution usually adopted for spectral classification, these weaker helium lines went unnoticed. We note in passing that a similar fraction ($\gtrsim$10%) of subdwarfs among cataloged "DAs" has been also found by other investigators in completely unrelated samples.

The BGRD sample of 45 genuine WDs (i.e., excluding subdwarfs and the two WD + RD pairs) was enlarged with seven additional DA WDs, leading to a set of 52 well observed, *confirmed* DA WDs, which constitute a very homogeneous sample in terms of the uniform data acquisition and reduction techniques. The 11 WDs in common with BSL[2] allow a cross check of the results that were obtained from the two independent data sets. For the two WD + red dwarf pairs the light contamination by the red dwarf companion makes more uncertain the derived WD atmospheric parameters; these two objects are discussed separately in § 6.2.

Figure 1 shows the distribution in V-magnitude, taken from the literature, for the 52 WDs in the ESO sample, plus the two WDs in the WD + RD systems. The comparison with the BSL sample indicates that the latter extends to fainter apparent magnitudes. Figure 2 compares the absolute magnitude distributions of the two samples (obtained by the model fitting technique, see § 3.1), showing that the ESO sample includes somewhat older and cooler objects than the BSL sample, spanning magnitudes from about 8.5 to 13.7, or cooling times from about 1.8×10^6 to 1.7×10^9 years (Green 1980). Apart from these differences, the two samples are otherwise substantially homogeneous. A discussed in §§ 3.3 and 5, cooler WDs need to be considered separately, while we believe that the slightly different luminosity functions of the two samples do not introduce a significant bias.

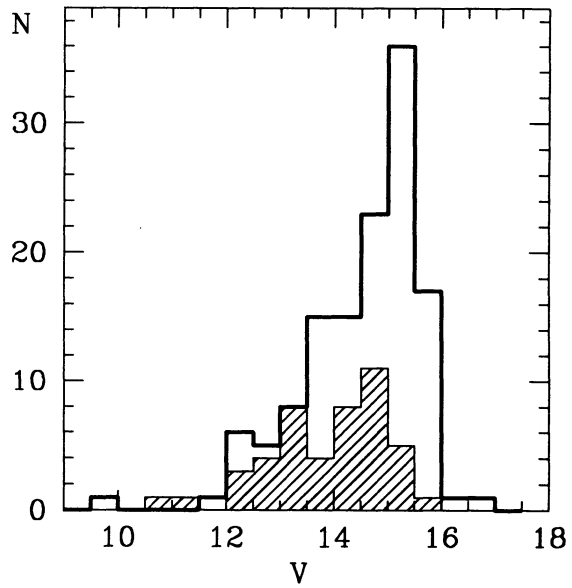

FIG. 1.—Distribution in apparent V-magnitude of the ESO (54 WDs; *shaded area*) and BSL samples (129 WDs; *thick line*).

2.2. *Observations*

The data analyzed here were collected in the period 1985–1991 at the ESO 3.6 m telescope mounting EFOSC (the ESO Faint Object Spectrograph and Camera) and the 1.52 m telescope equipped with a Boller & Chivens spectrograph. Various CCD detectors were used during the nine observing runs. For each star, we obtained at least two spectra; a narrow slit was used, usually 1″ at the 3.6 m telescope and 2″ at the 1.52 m.

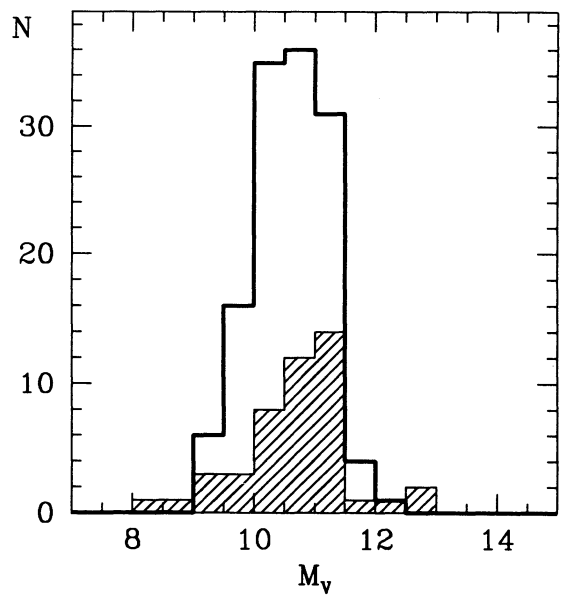

FIG. 2.—Distribution in absolute V-magnitude of the ESO (47 WDs; *shaded area*) and BSL sample (129 WDs; *thick line*). Only the WDs hotter than 12,000 K are plotted, including the hot component of the WD + RD pair 0034−211.

[2] Namely: 0346−011 (GD 50), 0612+177 (G 104−27), 1052+273 (GD 125), 1105−048 (G 163−50), 1327−083 (Wolf 485A), 1451+006 (GD 173), 1615−154 (G 153−41), 1845+019 (Lanning 18), 2039−202 (L 711−10), 2149+021 (G 93−48), 2204+071 (PG).

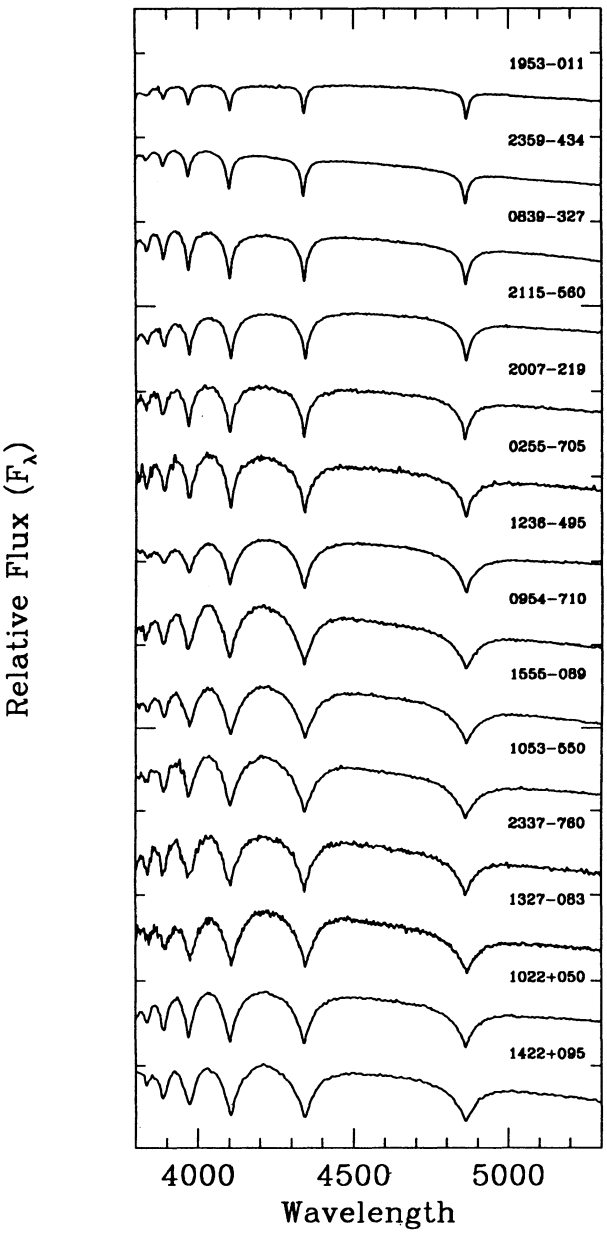

FIG. 3a

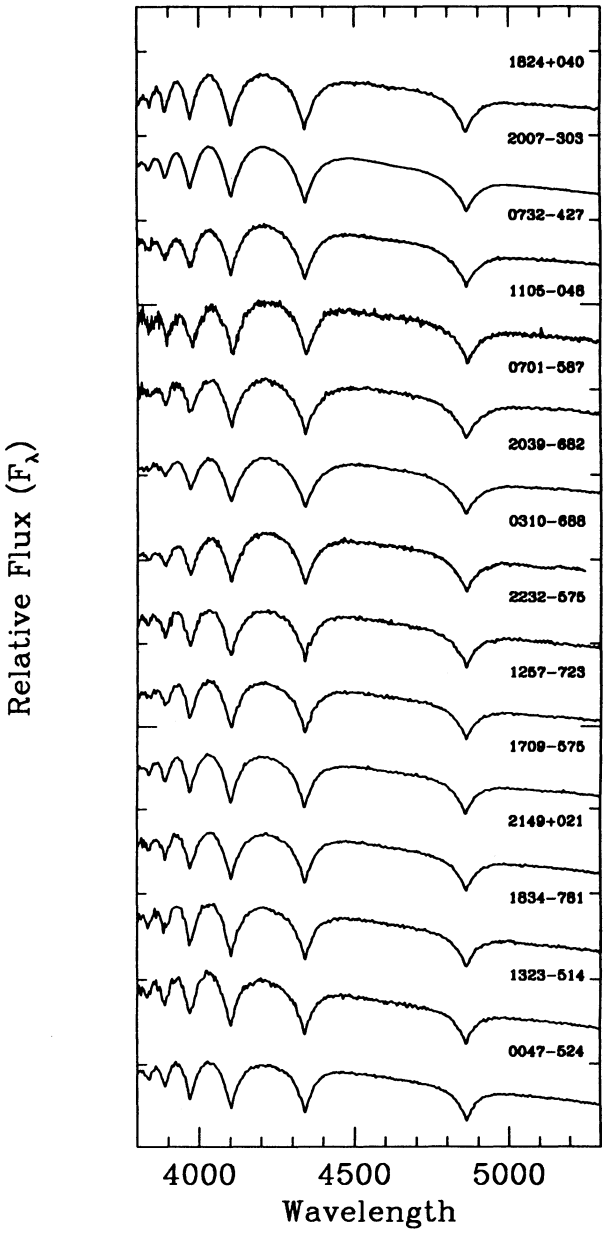

FIG. 3b

FIG. 3.—Complete ESO sample of DA WDs. (*a*, *b*, *c*): one spectrum is plotted for each object, in order of increasing $T_{\rm eff}$. The ordinate scale is in flux units, normalized between 4400 and 4600 Å. (*d*) The spectra of the two WD + RD pairs are shown separately, on an arbitrary scale.

Each WD in every observing run was also observed at least once with a larger slit, 5″ or 10″ respectively, which was used for the spectrophotometric standard stars as well. As a rule, the slit was aligned with the direction of the atmospheric refraction.

The spectral coverage is usually 3500–5500 Å, at a intermediate resolution of about 6 Å, an optimal choice to cover all Balmer lines from Hβ to H9. One or two calibration lamps (helium or helium-argon) were taken next to each exposure. A total of 288 spectra for the 52 WDs in the present sample were obtained. Their high quality (S/N $\sim$ 100) suggested their further use to derive the WD parameters, i.e., temperatures and surface gravities.

A representative spectrum for each WD is presented in Figure 3.

2.3. *Reductions*

The spectra have been reduced twice: first at ESO Headquarters using the standard IHAP procedure for the wavelength calibration, which was adequate for the radial velocity inspection of the spectra, the primary goal of our observations. Then all the spectra were reduced again, using the IRAF packages at the Lunar & Planetary Laboratory (University of Arizona), where the flux calibration was also performed. All frames have been bias subtracted and corrected for flat-field (and illumination when applicable). As a result of the narrow

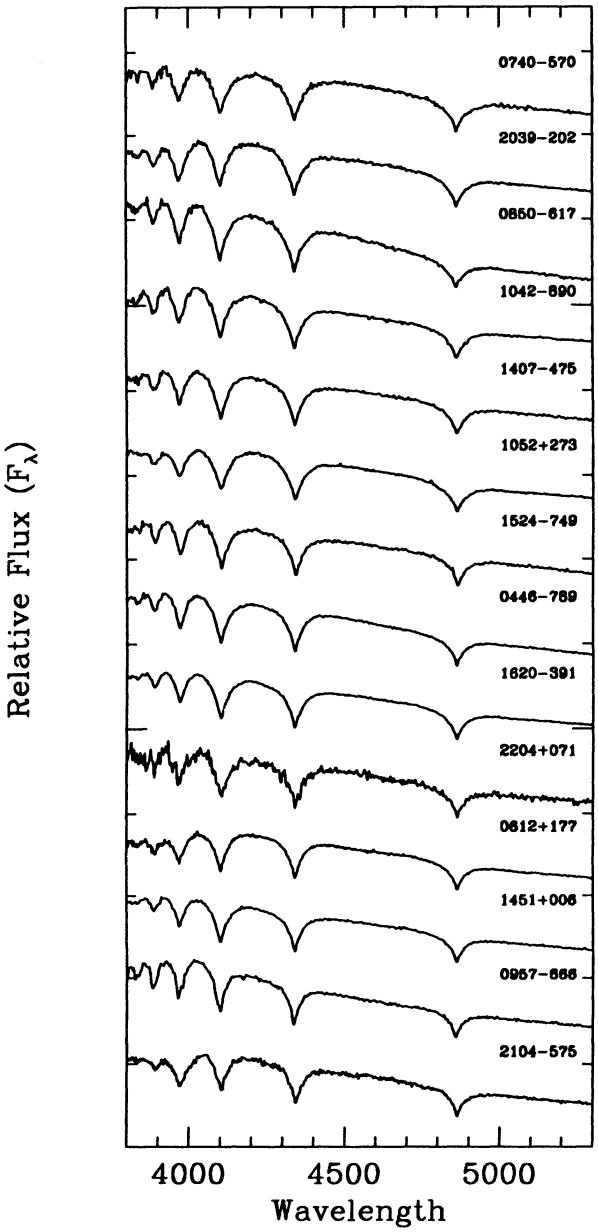

FIG. 3c

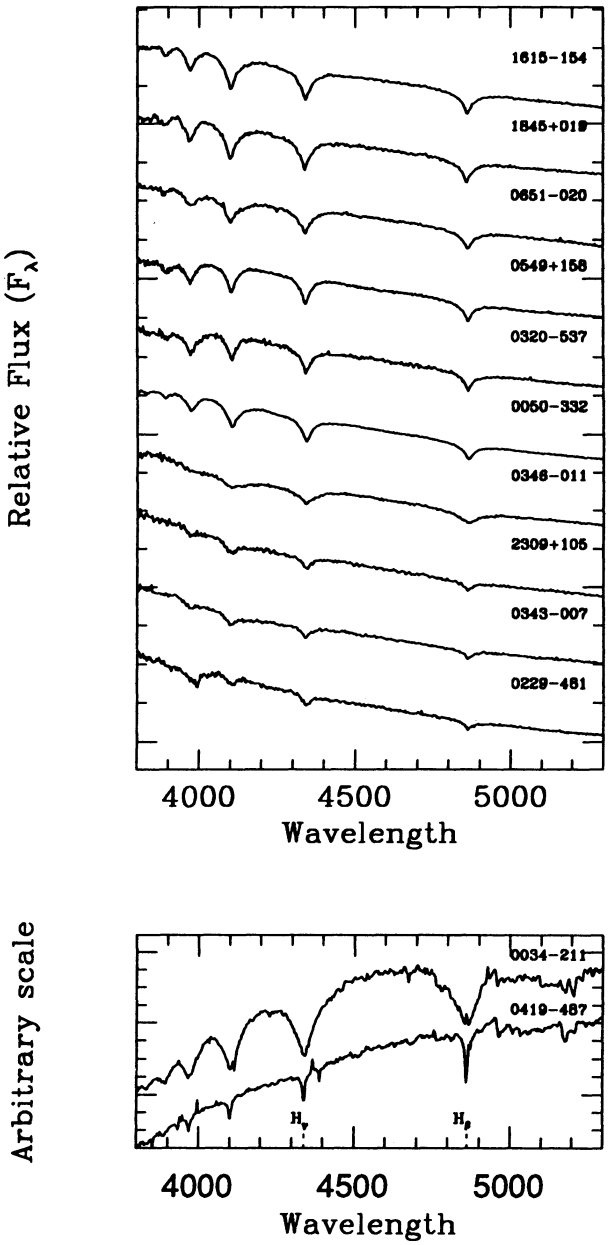

FIG. 3d

slit (1″ or 2″) used in the vast majority of observations, the flux calibration is not always of the best quality. On the other hand, we have at least one spectrum for each WD obtained with a slit large enough to collect all the light from the star even in bad seeing conditions and/or in case of not perfect centering of the star. Fortunately, the atmospheric parameters derived from spectra obtained with different slits are in good agreement with each other. Indeed, as detailed below, the fitting method used to derive $T_{\rm eff}$ and log g does not make use of the continuum shape but only of the line profiles, thus minimizing the effect of any imperfect flux calibration.

We finally note that, given the main goal of the project, we have from a minimum of 2 up to about 30 spectra of each WD (with an average of 5). Our results can then be used to assess the consistency of the method, and *external errors* of the derived values can be estimated.

3. DATA ANALYSIS AND RESULTS

3.1. *The Models*

The model spectra used here are those extensively described in BSL and references therein. The atmospheric parameters, $T_{\rm eff}$ and log g, are obtained by fitting the normalized Balmer line profiles (from Hβ to H9) to a grid of pure-hydrogen model atmospheres extending from 5000 to 100,000 K in $T_{\rm eff}$ and from 7.0 to 9.5 in log g. Use of all lines ensures a high degree of accuracy both in temperature and surface gravity determinations. The fitting technique has been applied to the complete original set of data, comprising the then rejected subdwarfs; more than 300 spectra were examined, and 288 retained for the confirmed DAs. For each spectrum, values of $T_{\rm eff}$ and log g are obtained along with the corresponding uncertainties of each fitted parameter, which represent a 1 σ estimate of the capabil-

ity of the models to fit accurately the data. These *internal errors* are typically of the order of 100–300 K in $T_{\rm eff}$ and 0.02–0.04 in log g. As discussed by BSL, the dominant source of error remains the flux calibration, even though the normalized line profiles, and not the continuum, are used in the fitting procedure. Bergeron (1993) studied in detail the internal consistency of the atmospheric parameters derived from individual Balmer lines. Furthermore, BSL compared the spectroscopic masses with those obtained from gravitational redshift measurements, and found an excellent agreement between both methods.

Figure 4 shows a few representative fits in order of decreasing effective temperatures. These include one of the hottest star in our sample (0343−007), the DD discovered by BGRD (0957−666), two low-mass objects which are most likely DD candidates as discussed in § 6.1 (1022+050 and 1824+040), the newly reported ZZ Ceti variable (1236−495), two of the coolest white dwarfs in our sample (2359−434 and 1953−011), two garden variety stars with normal masses (2014−575 and 0850−617), and a massive one (2039−682) whose spectrum can be contrasted with that of 1824+040 at a comparable temperature but much lower surface gravity.

The individual WD masses were obtained from the evolutionary models of Wood (1990), which span the range 0.4 to 1.2 $M_\odot$; additional carbon sequences at 0.2 and 0.3 $M_\odot$ have been kindly provided by M. A. Wood for the purpose of this analysis. These models take into account finite-temperature effects, so no mass underestimate due to noncomplete degeneracy at high $T_{\rm eff}$ and/or at low mass is present (for a discussion see, e.g., Koester & Schönberner 1986 and BSL). The WD models used have pure carbon cores, surrounded by a He layer of $10^{-4}\,M_*$ but no H layer. The particular choice of the models used (e.g., either a C—O core, or a different thickness of the He layer, or a thin H layer) seems to be rather irrelevant, but the resulting WD masses would be somewhat underestimated by $\sim 0.04\,M_\odot$ if these stars have thick (e.g., $\sim 10^{-4}\,M_\odot$) hydrogen layers (BSL).

Also, the mass of the low surface gravity objects should be estimated from evolutionary models with helium-core configurations if these stars are indeed the result of close binary evolution. But as discussed in BSL, a comparison of the zero-temperature mass-radius relations of Hamada & Salpeter (1961) indicates that there are no significant differences between the carbon and helium configuration models at $M \sim 0.3\,M_\odot$. Unfortunately, finite-temperature effects cannot be estimated because of the lack of extensive evolutionary models with helium cores published in the literature (see Iben & Tutukov 1986, however), although these effects are expected to be small if the stars are cool enough.

3.2. *Adopted Values and Errors*

Table 1 gives for each star the derived values of temperature, gravity, mass and absolute magnitude, along with identifications and V magnitudes taken from the literature. Also report-

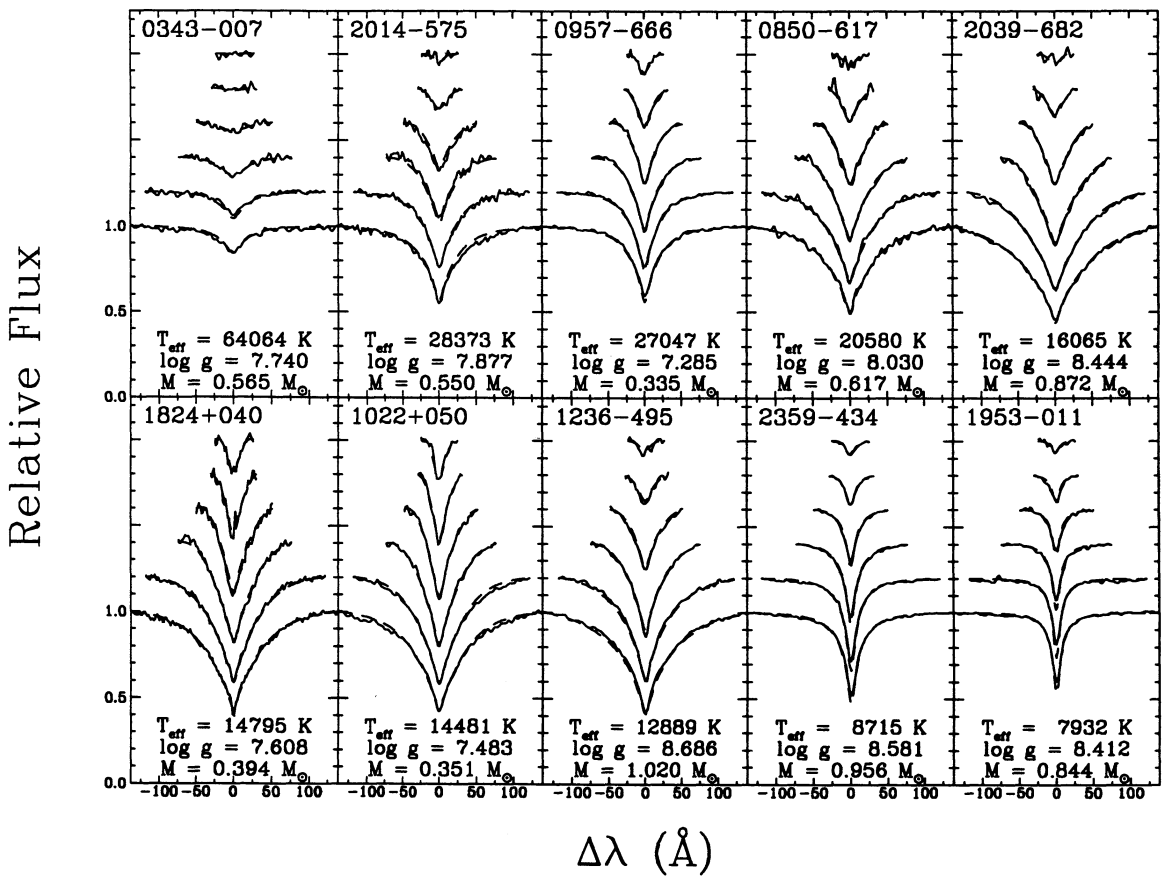

FIG. 4.—Fits to the individual Balmer lines for a representative subsample of program objects. The lines range from Hβ (*bottom*) to H9 (*top*), each offset vertically by a factor of 0.2. These objects are discussed in the text.

TABLE 1

TEMPERATURES, GRAVITIES, MASSES, AND ABSOLUTE MAGNITUDES OF THE PROGRAM WHITE DWARFS

WD	Name	V	n	$T_{\rm eff}$ (K)	$\sigma_{T_{\rm eff}}$	log g	$\sigma_{\log g}$	$M/M_\odot$	σ_M	M_V	Notes
0047−524	BPM16274	14.20	13	18745	564	7.830	0.050	0.504	0.026	10.71	1,3,10
0050−332	GD659	13.36	1	34980		7.991		0.619		9.73	5,1,3,8,9,10
0229−481		14.52	2	77421	2550	7.549	0.064	0.542	0.018	8.08	9,10
0255−705	BPM2819, LHS1474	14.08	2	11006	98	8.037	0.074	0.603	0.045	11.97	1,3
0310−688	EG21	11.40	6	16181	269	8.062	0.051	0.627	0.030	11.29	1,3,10
0320−539	LB 1663	14.50	1	34946		7.673		0.472		9.24	8,10
0343−007	KUV	14.91	3	64064	2601	7.740	0.107	0.565	0.038	8.56	
0346−011	GD50	13.98	11	43102	1982	9.092	0.090	1.225	0.080	11.45	3,5,6,9,10
0446−789	BPM3523	13.47	4	23614	78	7.825	0.041	0.514	0.020	10.28	
0549+158	GD71	13.06	3	33753	258	7.664	0.056	0.466	0.022	9.28	3,5,9,10
0612+177	G104-27	13.40	3	25938	369	7.973	0.124	0.597	0.068	10.31	1,2,3,5,6,10
0651−020	GD80	14.82	3	33697	270	8.170	0.087	0.721	0.052	10.07	3,5,9,10
0701−587	BPM18398	14.46	4	15701	694	8.562	0.191	0.944	0.115	12.11	3
0732−427	BPM33039, LHS1927	14.16	3	15298	60	8.080	0.031	0.635	0.019	11.42	1,3
0740−570	BPM18615	15.06	3	20273	168	8.179	0.054	0.705	0.033	11.07	1,3
0839−327	LTT3218	11.90	17	9393	76	7.955	0.107	0.553	0.063	12.41	2,3
0850−617	BPM5109	14.73	3	20580	96	8.030	0.029	0.617	0.017	10.83	1,3
0954−710	BPM6082	13.48	9	13915	155	7.722	0.037	0.449	0.040	11.10	1,3,10
0957−666	BPM6114	14.60	26	27047	398	7.285	0.082	0.335	0.018	9.14	1,3
1022+050	LP550-052, PG	14.18	7	14481	341	7.483	0.164	0.351	0.058	10.68	3,10
1042−690	BPM6502	13.09	2	21380	258	7.864	0.030	0.528	0.014	10.52	1,3,10
1052+273	GD125	14.12	3	23377	326	8.269	0.034	0.767	0.022	10.96	1,3,5,6,10
1053−550	LTT4013	14.32	3	14178	35	7.897	0.045	0.528	0.024	11.30	1,3
1105−048	G163-050	12.92	3	15576	130	7.805	0.050	0.484	0.025	11.00	1,2,3,6,10
1236−495	LTT4816	13.96	9	12899	740	8.686	0.115	1.020	0.065	12.72	1,3,10
1257−723	BPM7961	15.18	3	17001	416	8.009	0.033	0.598	0.019	12.63	3
1323−514	BPM21970, LHS2737	14.60	2	18713	420	7.870	0.019	0.525	0.011	10.77	1,3
1327−083	Wolf485A	12.30	3	14413	180	7.847	0.032	0.502	0.017	11.20	1,2,3,4,6,10
1407−475	BPM38165	14.31	4	22286	544	7.812	0.044	0.504	0.023	10.38	1,3
1422+095	GD165	14.32	2	14618	398	7.856	0.064	0.507	0.035	11.19	3, 7
1451+006	GD173	15.29	4	26371	110	7.926	0.086	0.572	0.043	10.21	3,6
1524−749	BPM9518	15.93	3	23541	532	7.756	0.034	0.481	0.014	10.19	3
1555−089	G152B4B	14.80	3	14133	111	7.880	0.044	0.519	0.023	11.28	1,2,3
1615−154	G153-41	13.42	3	29833	42	8.083	0.039	0.663	0.023	10.18	1,3,5,6,10
1620−391	GR274	11.00	7	24406	328	8.099	0.038	0.664	0.023	10.63	1,3,5,10
1709−575	BPM24273	15.10	3	17130	209	7.956	0.051	0.569	0.028	11.04	1,3
1824+040	G21-15	13.90	5	14795	389	7.608	0.068	0.394	0.027	10.83	1,3,4
1834−781	BPM11593	15.45	3	17792	338	7.903	0.059	0.541	0.033	10.91	3
1845+019	Lanning 18	12.96	15	30352	404	7.832	0.118	0.534	0.058	9.75	5,6,9,10
1953−011	G92-40, LTT7879	13.70	3	7932	25	8.412	0.053	0.844	0.035	13.77	1,2,3,4,10
2007−219	LTT7983	12.40	6	10021	117	8.180	0.081	0.692	0.052	12.49	1,3
2007−303	LTT7987	12.18	19	15152	320	7.861	0.048	0.512	0.025	11.13	10
2014−575	L210-114	13.00	3	28373	467	7.877	0.045	0.550	0.022	9.98	9,10
2039−202	L 711-10	12.34	3	20416	280	7.841	0.045	0.514	0.022	10.57	1,3,5,6
2039−682	LTT8190	13.53	3	16065	226	8.444	0.024	0.872	0.016	11.89	1,3
2115−560	LTT8452	14.28	3	9944	5	8.128	0.037	0.658	0.024	12.44	1,3
2149+021	G93-48	12.73	3	17653	319	7.994	0.068	0.592	0.040	11.05	2,3,4,6,10
2204+071	PG	15.86	1	24623		7.980		0.595		10.43	6, 8
2232−575	BPM27891	14.96	3	16435	488	7.931	0.036	0.553	0.020	9.25	3
2309+105	GD246	13.10	2	57990	2103	8.073	0.057	0.697	0.028	11.08	1,4,5,9,10
2337−760	BPM15727	14.66	3	14295	144	7.507	0.016	0.354	0.005	10.75	
2359−434	LTT9857	13.05	2	8715	8	8.581	0.032	0.956	0.021	13.70	1,2,10

NOTES.—$T_{\rm eff}$, log g, and M found also in: (1) KSW; (2) Shipman 1979; (3) Guseinov et al. 1983; (4) McMahan 1989; (5) only $T_{\rm eff}$ and log g: Kidder 1991; (6) BSL; (7) Observed at lower resolution; (8) See text for internal errors; (9) Detected by *ROSAT*; (10) Observed by *IUE*.

ed are the number of spectra used for the analysis (n), and the standard deviations ($\sigma_{T_{\rm eff}}$, $\sigma_{\log g}$, σ_M) from the mean value of $T_{\rm eff}$, log g and mass (each being the average of the n derived values). We excluded from the average the results obtained from the worse S/N spectra and from the poorest fits. Only in three cases (0050−332, 0320−537, 2204+071) this left us with only one usable spectrum for the analysis. The internal errors in $T_{\rm eff}$ and log g for the three WDs with only one spectrum available are respectively: 91 K, 0.016 (0050−332); 326 K, 0.058 (0320−537); 579 K, 0.074 (2204+071).

The σ's reported in Table 1 represent the *external errors* of the complete process, from data acquisition, to reduction and

analysis. They can be compared with the internal errors for the same object, which is a measure of the accuracy of the model atmosphere to fit the observed spectra; such a comparison is shown in Figure 5 for the 46 WDs hotter than 12,000 K (see later). External errors are generally comparable or larger than internal ones.

We now focus on the 46 WDs hotter than 12,000 K; the reason for this limit, different from the 15,000 K limit chosen by BSL, is given in § 3.3. Cooler WDs are also discussed in § 3.3. The average values of the external errors obtained from multiple measurements are $\langle\sigma_{T_{\rm eff}}\rangle = 490$ K (but it decreases to 270 K excluding the three very hot WDs), $\langle\sigma_{\log g}\rangle = 0.06$, $\langle\sigma_M\rangle = 0.03\ M_\odot$. About 75% of the 46 WDs have $\sigma_T < 500$ K and 25% have $\sigma_{T_{\rm eff}} < 200$ K. We note that in the few cases where the resulting $\sigma_{T_{\rm eff}}$ is unrealistically low, the relative internal error or the mean $\sigma_{T_{\rm eff}}$ derived for the whole sample may be assumed as a better error estimate. Standard deviations in log g are less than 0.06 for about 65% of the DAs. Figure 6 shows the relative external errors $\sigma_X/\langle X\rangle$ as a function of X. No trend is noticeable in the relative errors. In practice, 85% of the DA stars have errors less than 3% in $T_{\rm eff}$, 1.5% in log g, and 8% in mass.

BSL observed 17 WDs twice and one WD three times so as to check the reliability of the method. The mean derived errors are: $\langle\Delta T_{\rm eff}\rangle = 350$ K, $\langle\Delta \log g\rangle = 0.049$, and $\langle\Delta M\rangle = 0.03\ M_\odot$, values similar to our mean external errors and to their (and our) internal errors. We may therefore conclude that the present sample of 46 hot WDs is comparable in quality to the BSL sample, and the derived WD parameters have quite similar accuracy (see § 4 for a discussion and direct comparison).

Finally, Figure 7 shows the distribution of all objects in the $T_{\rm eff}$–log g plane where errorbars represent the external errors for the 43 hot WDs with multiple measurements, and the associated internal errors for the three WDs with a single spectrum, shown with a different symbol. Also plotted are the evolutionary models of Wood (1990) for various masses, from 0.4 to 1.2 $M_\odot$, with carbon-core composition, a He layer of $10^{-4}\ M_*$ (10^{-5} for 1 and 1.2 $M_\odot$) and no hydrogen, and the cooling sequences of Koester & Schönberner (1986) with and without a $10^{-4}\ M_\odot$ hydrogen envelope.

3.3. *The Cool White Dwarfs*

Bergeron et al. (1994) have determined the atmospheric parameters for a sample of 18 ZZ Ceti stars, and have shown that the ML2 parameterization of the mixing-length theory (see Bergeron, Wesemael, & Fontaine 1992) yields a mass distribution which is consistent with that of hotter stars; this calibration is used in the present analysis. This result allows us to include in our mass distribution stars cooler than the 15,000 K cutoff used by BSL.

However, Bergeron, Wesemael, & Fontaine (1991) have shown that below $T_{\rm eff} \sim 12{,}000$ K it is not possible to separate the pressure effects on the Balmer lines originating from an increased helium abundance from those stemming from an increased surface gravity. Since helium is spectroscopically invisible at these temperatures, a high log g object can be interpreted as a helium-enriched star with a lower surface gravity. On the basis of their models, Bergeron et al. (1990) have shown that most WD stars below $T_{\rm eff} \sim 12{,}000$ K have helium-enriched atmospheres as most objects appeared to have larger than average surface gravities, a result which has been interpreted as evidence of mixing between the hydrogen convection zone and the more massive underlying helium layer. These results also imply that for cool WDs it is not possible to uniquely determine the surface gravity (or the mass). Although the conclusions of Bergeron et al. (1990) are still a subject of discussion, we prefer to exclude from this analysis all stars cooler than 12,000 K until a complete understanding of the chemical composition of cool white dwarfs becomes available. Nevertheless, we note that most, but not all, stars cooler than 12,000 K in Table 1 do indeed possess surface gravities that are larger than the average value. The mean value of the mass for these six cool objects is 0.717 $M_\odot$.

4. COMPARISON WITH PREVIOUS WHITE DWARF STUDIES

Before proceeding with the discussion of the derived WD masses, a comparison with the results of the previous investigations reported in § 1 is appropriate. Since our sample includes essentially the brightest WDs visible in each observing run, it is not surprising that many of them had already been observed several times. Some of the hotter stars ($T_{\rm eff} \gtrsim 30{,}000$ K) have

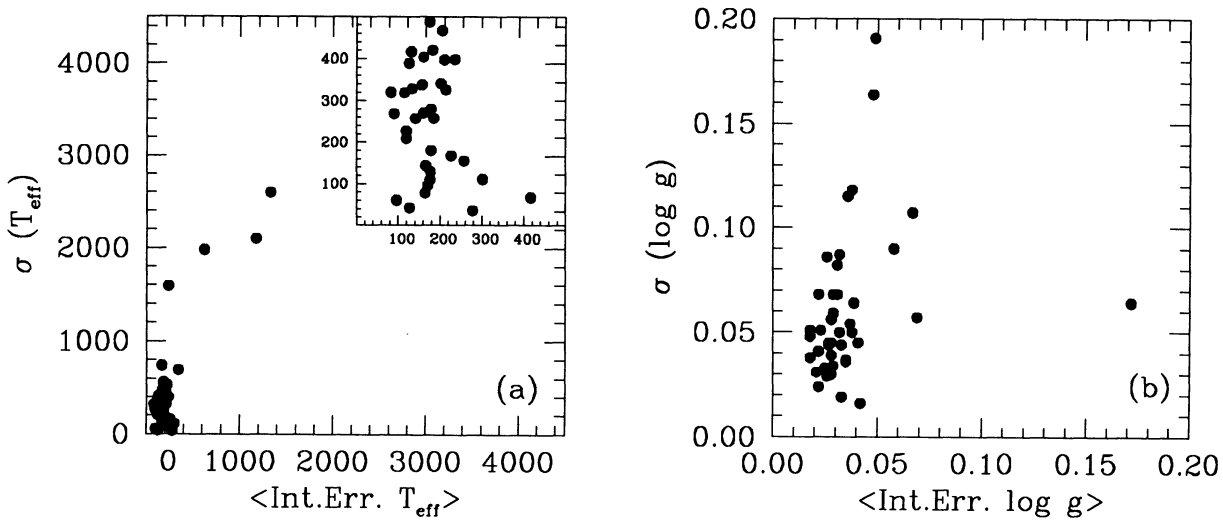

FIG. 5.—Star by star comparison of the mean internal errors in $T_{\rm eff}$ (*a*) and log g (*b*) with the corresponding σ-values. The left panel also shows an enlargement with a better resolution.

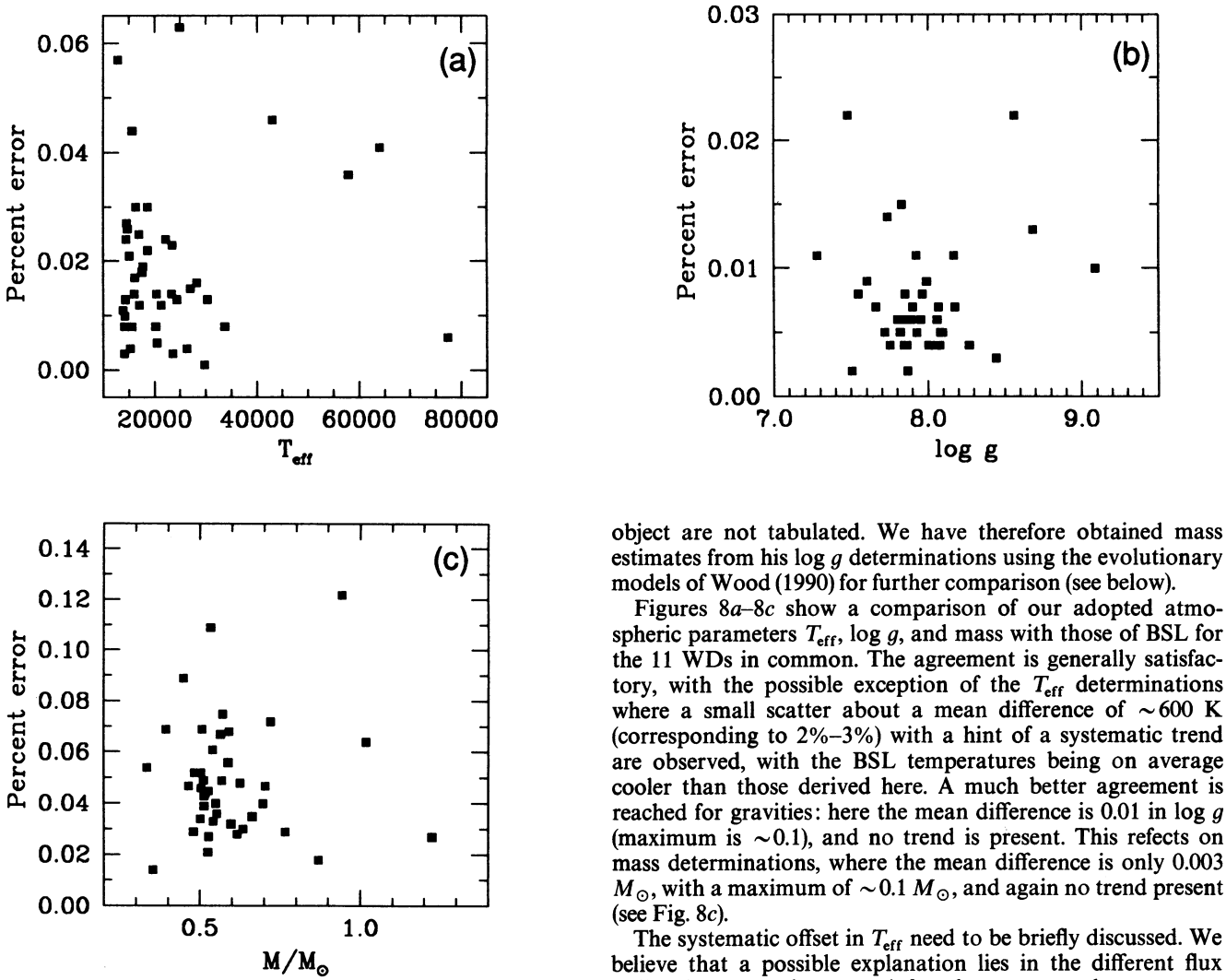

FIG. 6.—Percent errors in T_{eff} (*a*), log g (*b*), and mass (*c*) for the 46 "hot" WDs.

also been detected by *ROSAT* (Wide Field Camera all-sky survey; Pounds et al. 1993) and some have been observed by the *IUE* satellite, as a search of the archive showed (see Table 1).

The largest overlap is with KSW with 30 objects in common; eight WDs are in common with Shipman (1979), six with McMahan (1989), 12 with Kidder (1991) and 11 with BSL. Note that our analysis is essentially a survey of the Southern sky, while almost all the 70 WDs studied by Weidemann & Koester (1984) are confined to the northern hemisphere, so we have only one star in common and no significant star-by-star comparison is possible with their sample. For stars in common with previous studies, we compare in Table 2 the values of the temperatures, surface gravities, and masses with our own determinations. All the above studies have been examined and compared by BSL, except for the results of Kidder (1991) who observed 102 hot DA WDs, and derived T_{eff} and log g-values from UV and optical spectra using an extension of the Wesemael (1980) models, and fitted the line profiles of Lyα, Hβ, Hγ, and Hδ. Although Kidder (1991) presents a mass distribution for his sample, the individual mass determinations for each object are not tabulated. We have therefore obtained mass estimates from his log g determinations using the evolutionary models of Wood (1990) for further comparison (see below).

Figures 8*a*–8*c* show a comparison of our adopted atmospheric parameters T_{eff}, log g, and mass with those of BSL for the 11 WDs in common. The agreement is generally satisfactory, with the possible exception of the T_{eff} determinations where a small scatter about a mean difference of $\sim$600 K (corresponding to 2%–3%) with a hint of a systematic trend are observed, with the BSL temperatures being on average cooler than those derived here. A much better agreement is reached for gravities: here the mean difference is 0.01 in log g (maximum is $\sim$0.1), and no trend is present. This refects on mass determinations, where the mean difference is only 0.003 $M_{\odot}$, with a maximum of $\sim$0.1 $M_{\odot}$, and again no trend present (see Fig. 8*c*).

The systematic offset in T_{eff} need to be briefly discussed. We believe that a possible explanation lies in the different flux calibration procedures used for the two samples, a consequence of how data were collected. While BSL observed their WDs with the primary purpose of obtaining accurate temperatures and gravities, WDs analyzed in this study were primarily observed for radial velocity studies. This means that the two observing strategies were optimized to reach the best flux collection (BSL) or the best spectral and time resolution (BGRD). On average, BSL flux calibrations are probably somewhat more accurate than those in BGRD.

Combining the external errors of the samples (350 K for BSL and 490 for this work), differences between temperatures are significative if above about 600 K. If we do a star-by-star comparison, the worst cases are represented by GD 173 with about 700 K, WD 2204+071 with about 1000 K, and GD 50 for which the difference is about 2500 K ($\sim$6%). About GD 173, the four flux calibrated spectra show differences, but we were unable to choose unequivocally the best one, so we retained all four, though we were aware of so lowering the precision of the derived parameters. For WD 2204+071 the difference is easily explained by the very low S/N in our spectrum; indeed, when later combining values for the samples, we use the BSL value. Finally, GD 50, the highest temperature in the BSL sample, has weak features; furthermore, while most of the spectra used in this analysis have lower S/N, the one used in BSL suffered from a glitch in the Hγ line.

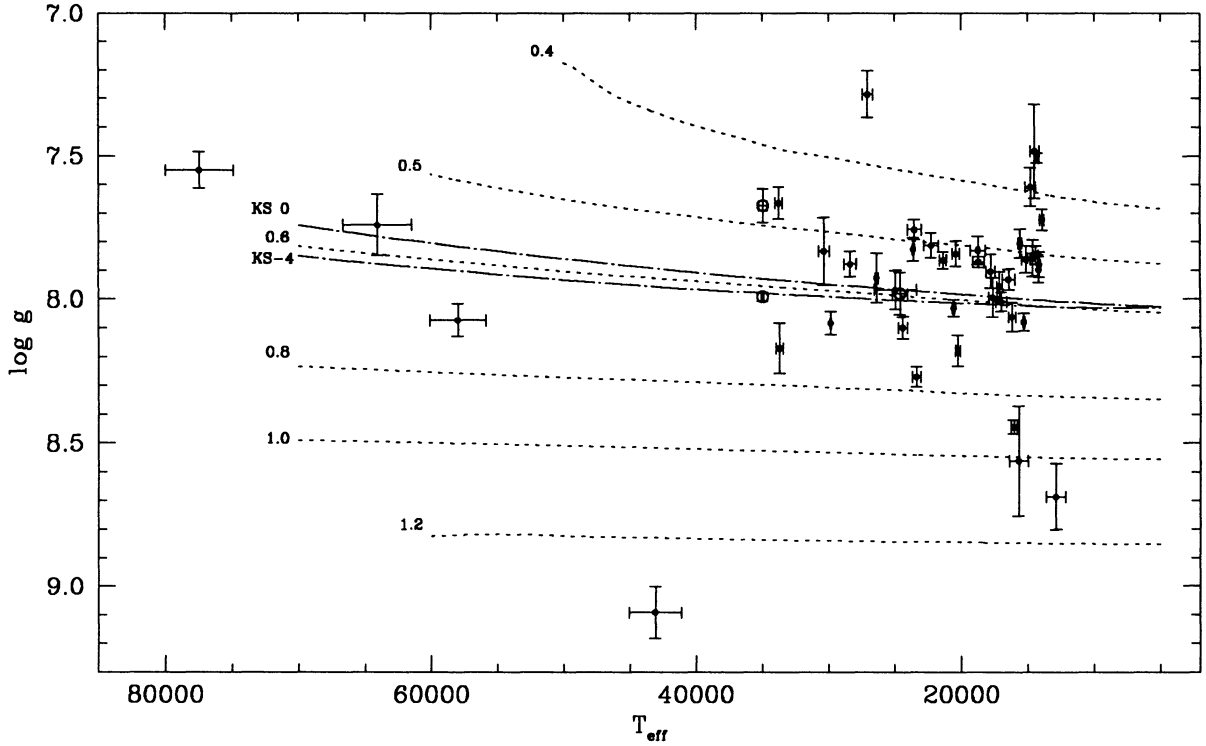

FIG. 7.—Surface gravities as a function of effective temperatures for the 43 WDs with multiple measurements (*small dots*) and associated 1 σ external errors, and for the three stars with only one measurement (*open circles*) and 1 σ internal errors. Some of the evolutionary models of Wood (1990) are displayed, for $M = 0.4$ to 1.2 $M_\odot$ (*dashed lines*). The dash-dotted lines represent the 0.598 $M_\odot$ models of Koester & Schönberner (1986) with 0 and 10^{-4} $M_\odot$ hydrogen-rich envelopes, as indicated.

The comparison with all other results is shown in Figures 9*a*–9*c*. Temperatures differ generally by less than 10% and no systematic trend is observed. For log g's (Fig. 9*b*) there is, instead, such a trend with our determinations being systematically larger than those derived from photometry (see for example KSW, where this is true for 27 WDs out of 30), while not systematic effects are present for the ones derived from spectroscopic data (e.g., Kidder 1991). This reflects heavily on mass determinations as well (Fig. 9*c*). Furthermore, masses in previous investigations were derived from the zero-temperature Hamada-Salpeter mass-radius relation while ours (and those of Kidder 1991, as discussed above) are obtained from the evolutionary models of Wood (1990). This can lead to an additional mass uncertainty as discussed by BSL.

There is a particularly good agreement in the log g distributions between this analysis and those of BSL and Kidder (1991), as can be seen in Figure 10. All distributions are characterized by a sharp peak located in the same range of log g, and also display extended tails at both high and low values of log g. The main conclusion of this comparison is, as already found by BSL, that gravities (and masses) derived from spectral line fits show very good agreement, while major deviations are present when the comparison is made with gravities obtained from broad- or narrow-band colors and spectrophotometric indices (Fig. 9). CCD spectroscopy coupled to model atmosphere fits clearly yields superior results.

5. THE MASS DISTRIBUTION

Figure 11 shows the comparison of the mass distribution of the 46 hot WDs in our sample with that of BSL for their sample of 129 WDs. Both distributions are characterized by a steep rise at $M \simeq 0.5$ $M_\odot$ and extended tails toward high masses. These distributions, at first, look quite similar to that derived by e.g., Weidemann & Koester (1984). Note however the low mass hump ($M < 0.4$ $M_\odot$) definitely present in both distributions and currently attributed to binary born helium WDs (BSL; BGRD). This feature was absent in the Weidemann and Koester mass distribution, which led Weidemann (1990) to suspect a theoretical "overestimate" of the number of close binary-born WDs.

The distribution for the 46 WDs peaks at 0.50–0.55 $M_\odot$ (the mode), with a mean mass of 0.587 $M_\odot$ and a dispersion of 0.166 $M_\odot$, which compare to 0.562 and 0.137 $M_\odot$, respectively, for BSL. The average mass becomes 0.609 $M_\odot$ and the standard deviation 0.157 $M_\odot$, if we exclude the four objects with masses lower than 0.4 $M_\odot$, i.e., excluding confirmed or suspected binaries (e.g., 0957 − 666 has been identified as a DD system by BGRD). We also notice that roughly 10% of the objects appear to be binary-born He WDs, in agreement with the estimate of BGRD. In the BSL sample there are 11 WDs with $M \leq 0.4$ $M_\odot$; excluding them, their average mass becomes 0.582 $M_\odot$, with a dispersion of 0.124 $M_\odot$. Our distribution shows a moderate excess of objects between 0.6 and 0.7 $M_\odot$, which accounts for the different average masses. Indeed, a Kolmogorov-Smirnov test on the samples indicates no difference between the two distributions at the 90% confidence level.

Finally, combining our sample with that of BSL, spectroscopic determinations of $T_{\rm eff}$, log g, and mass become available for 164 field DA WDs. The corresponding mass distribution is shown in Figure 11*c*. For the 11 WDs in common, the values derived here have been adopted except for 2204 + 071, where a better fit is achieved with the higher S/N spectrum of BSL.

TABLE 2

COMPARISON WITH PREVIOUS ANALYSES

WD	$T_{\rm eff}$					log g					$M/M_\odot$				
	(1)	(2)	(3)	(4)	(5)	(1)	(2)	(3)	(4)	(5)	(1)	(2)	(3)	(4)	(5)
0047−524	19145					7.62					0.36				
0050−332	35759			36000		6.08			7.95					0.600	
0229−481															
0255−705	10596					7.86					0.49				
0310−688	15441					7.51					0.32				
0320−539				30700					7.52					0.406	
0343−007															
0346−011			34282	43400	40540			8.0	>9	9.22			0.585	>1.188	1.27
0446−789															
0549+158				33000					7.80					0.521	
0612+177	25164	26700		25800	24660	7.30	8.2		7.95	7.94	0.24	0.7		0.582	0.57
0651−020									8.00						
0701−587															
0732−427	14839					8.00					0.57				
0740−570	23876					7.36					0.26				
0839−327		9300					7.6					0.33			
0850−617	20776					7.84					0.48				
0954−710	14571					7.60					0.39				
0957−666	25250					6.87					0.13				
1022+050															
1042−690	20323					7.83					0.47				
1052+273	17354			23800	22750	7.80			8.50	8.41	0.45			0.915	0.86
1053−550	14432					7.78					0.44				
1105−048	15539	15300			15540	7.95	8.0			7.82	0.54	0.55			0.49
1236−495	13033					8.55					0.93				
1257−723															
1323−514	19062					7.72					0.41				
1327−083	14062	12800	16581		14350	8.24	7.7	8.04		7.92	0.59	0.41	0.592		0.54
1407−475	21558					7.61					0.36				
1422+095															
1451+006					25670					7.83					0.52
1524−749															
1555−089	13826	12600				7.60	7.6				0.39	0.34			
1615−154	43144			30200	29730	7.94			8.05	7.94	0.53			0.645	0.58
1620−391	24532			24800		7.39			8.25		0.27			0.757	
1709−575	17814					7.56					0.34				
1824+040	13822		13282			7.20		7.30			0.24		0.239		
1834−781															
1845+019				30000	29840				7.90	7.78				0.563	0.51
1953−011	8164	8200	8548			7.98	8.2	7.96			0.55	0.68	0.543		
2007−219	7475					7.58					0.35				
2007−303															
2014−575															
2039−202	19445			19500	19900	7.52			7.85	7.93	0.32			0.517	0.56
2039−682	16674					8.15					0.52				
2115−560	8954					7.92					0.52				
2149+021		18300	20547		18250		7.9	7.93		8.02		0.57	0.526		0.61
2204+071					23570					7.93					0.56
2232−575															
2309+105	65425		62213	56200		8.41		8.45	7.80		0.83		0.860	0.568	
2337−760															
2359−434	8131	18700				7.72	9.4				0.91	1.31			

NOTES.—(1) KSW; (2) Shipman 1979; (3) McMahan 1989; (4) Kidder 1991 (but masses derived by PB for this paper using Wood's models); (5) BSL.

We note that the two samples are not fully homogeneous, however, with the BSL sample being restricted to WDs hotter than ~15,000 K to avoid complications brought about by atmospheric convection (mixing length parameterization, helium dredge-up, etc.) which may affect surface gravity (mass) determinations of cooler stars. As discussed in § 3.3, we believe that gravities and masses here derived for stars with 12,000 $\lesssim T_{\rm eff} \lesssim$ 15,000 K are free from appreciable systematic errors with respect to hotter WDs. This makes legitimate the amalgamation of the two samples having excluded from the BGRD sample only the 6 DA stars with temperatures significantly lower than 12,000 K. With this proviso, the distribution of the

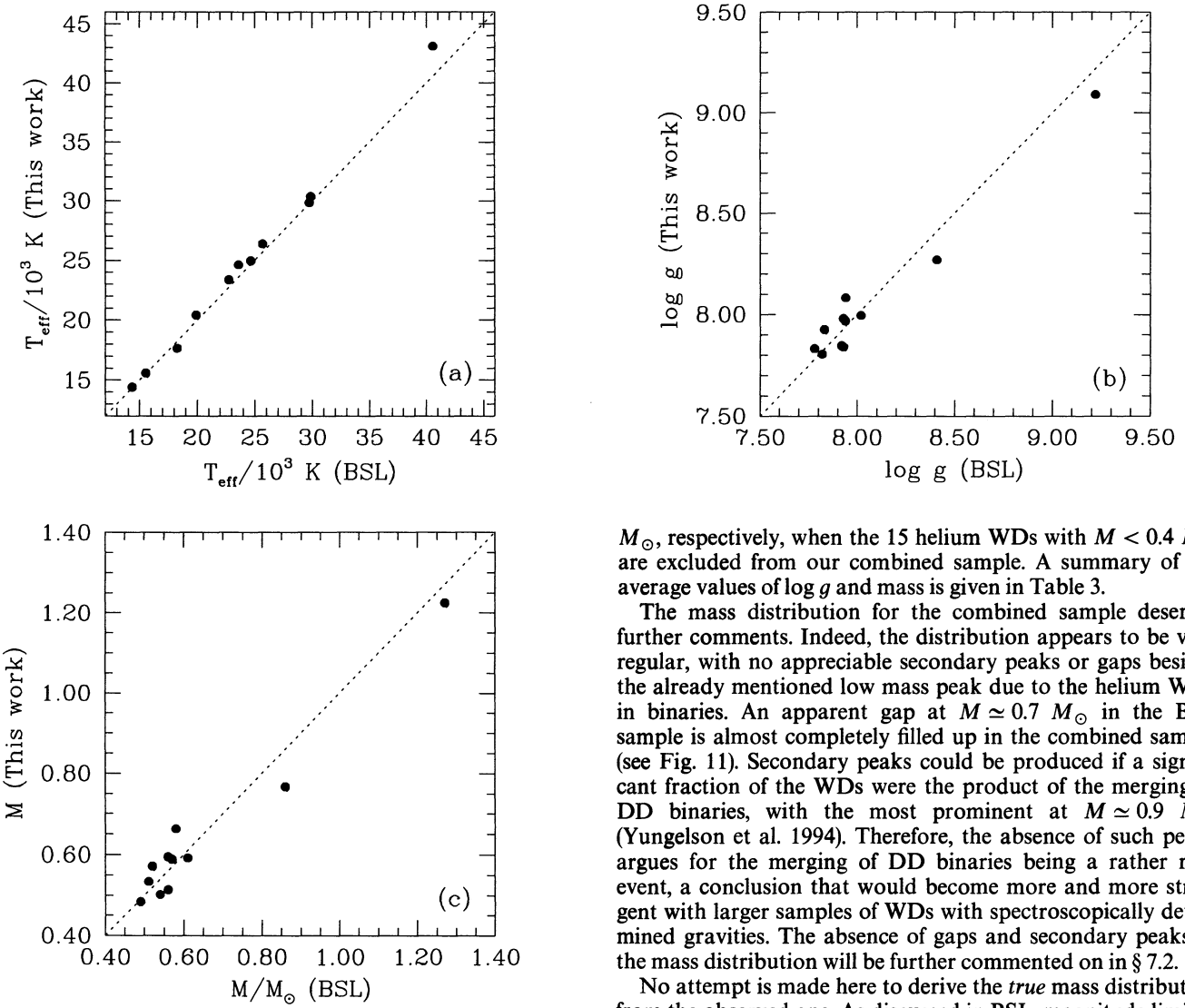

FIG. 8.—Comparison between the temperatures (*a*), gravities (*b*), and masses (*c*) in the present study and the results of BSL for the 11 WDs in common

combined sample is characterized by a mode between 0.50 and 0.55 $M_\odot$, and by an average mass of 0.566 $M_\odot$ and a dispersion of 0.136 $M_\odot$. These numbers are in excellent agreement with the values of 0.58 and 0.13 $M_\odot$, respectively, given by Weidemann & Koester (1984), though the accuracy of the present mass determinations is better. This ensures that no major systematic offset exits with such older mass determinations. Average mass and dispersion become 0.587 and 0.124 $M_\odot$, respectively, when the 15 helium WDs with $M < 0.4\ M_\odot$ are excluded from our combined sample. A summary of the average values of log g and mass is given in Table 3.

The mass distribution for the combined sample deserves further comments. Indeed, the distribution appears to be very regular, with no appreciable secondary peaks or gaps besides the already mentioned low mass peak due to the helium WDs in binaries. An apparent gap at $M \simeq 0.7\ M_\odot$ in the BSL sample is almost completely filled up in the combined sample (see Fig. 11). Secondary peaks could be produced if a significant fraction of the WDs were the product of the merging of DD binaries, with the most prominent at $M \simeq 0.9\ M_\odot$ (Yungelson et al. 1994). Therefore, the absence of such peaks argues for the merging of DD binaries being a rather rare event, a conclusion that would become more and more stringent with larger samples of WDs with spectroscopically determined gravities. The absence of gaps and secondary peaks in the mass distribution will be further commented on in § 7.2.

No attempt is made here to derive the *true* mass distribution from the observed one. As discussed in BSL, magnitude limited samples tend to be somewhat biassed against WDs of higher mass, as such WDs have higher densities, stronger neutrino losses, and therefore faster evolution through the upper part of the WD luminosity function.

6. SOME SPECIAL WHITE DWARFS

6.1. *Individual Objects*

In the following, we briefly comment on some individual WDs with special characteristics.

1. The WDs 0229−481, 0343−007 and 2309+105 are the

TABLE 3

AVERAGE VALUES FOR THE SAMPLES

	$T_{eff} > 12{,}000$ K			$T_{eff} > 12{,}000$ K; $M > 0.4\ M_\odot$		
Parameter	BSL (129 WDs)	ESO (46 WDs)	BSL + ESO (164 WDs)	BSL (118 WDs)	ESO (42 WDs)	BSL + ESO (149 WDs)
$\langle \log g \rangle$	7.910	7.943	7.911	7.954	7.988	7.958
$\sigma_{\log g}$	0.258	0.311	0.258	0.221	0.284	0.219
$\langle M/M_\odot \rangle$	0.562	0.587	0.566	0.582	0.609	0.587
σ_M	0.137	0.166	0.136	0.124	0.157	0.124

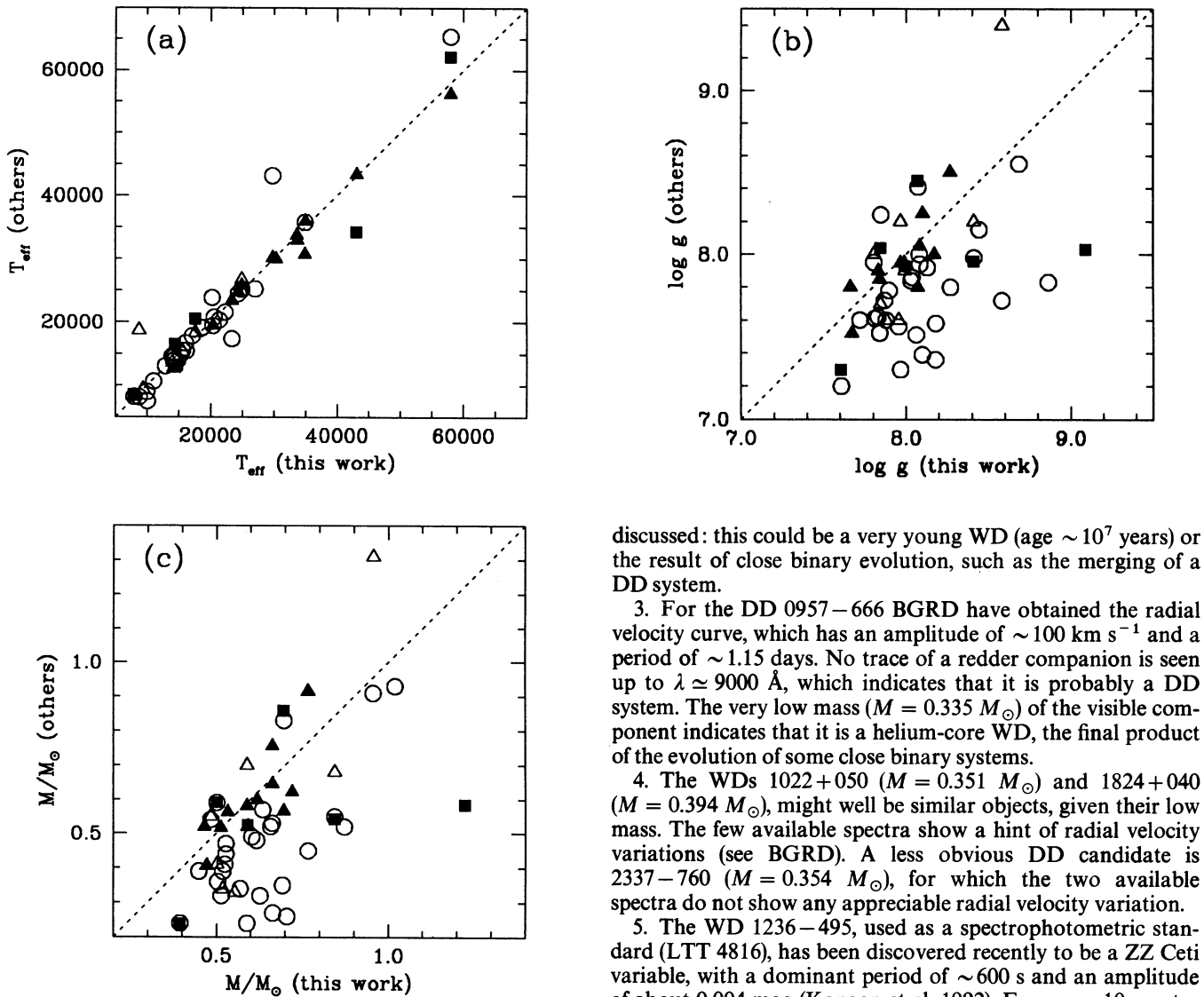

FIG. 9.—Comparison of our adopted atmospheric parameters $T_{\rm eff}$ (*a*), log g (*b*) and masses (*c*), with the results of KSW (*open circles*), Shipman (1979) (*open triangles*), McMahan (1989) (*filled squares*), Kidder (1991) (*filled triangles*).

hottest DAs in our sample, with temperatures of 76,000, 64,000, and 58,000 K, respectively. The spectrum of the first star, which turns out to be near the observed upper limits for DA WDs, is however rather noisy and the derived temperature is uncertain, with internal errors of the order of ~4200 K. The WDs 0229−481 (LB 1628) and 2309+105 (GD 246) have also been detected as bright EUV sources by *ROSAT* during its Wide Field Camera all-sky survey (Pounds et al. 1993).

2. The WD 0346−011 (the well-known star GD 50) is the most massive DA star in our sample ($M \sim 1.2 \pm 0.08\ M_\odot$), and therefore it plays an important role in establishing the upper mass limit for WDs. Unfortunately, the error in the derived mass is still fairly high, and further observations would be very important. Our determination is in rather good agreement with that of BSL, and with the high gravity estimated by Kidder (1991), but the WD is twice as massive as estimated by McMahan (1989). A detailed analysis of this object has been presented by Bergeron et al. (1991), where two hypotheses are discussed: this could be a very young WD (age $\sim 10^7$ years) or the result of close binary evolution, such as the merging of a DD system.

3. For the DD 0957−666 BGRD have obtained the radial velocity curve, which has an amplitude of ~100 km s^{-1} and a period of ~1.15 days. No trace of a redder companion is seen up to $\lambda \simeq 9000$ Å, which indicates that it is probably a DD system. The very low mass ($M = 0.335\ M_\odot$) of the visible component indicates that it is a helium-core WD, the final product of the evolution of some close binary systems.

4. The WDs 1022+050 ($M = 0.351\ M_\odot$) and 1824+040 ($M = 0.394\ M_\odot$), might well be similar objects, given their low mass. The few available spectra show a hint of radial velocity variations (see BGRD). A less obvious DD candidate is 2337−760 ($M = 0.354\ M_\odot$), for which the two available spectra do not show any appreciable radial velocity variation.

5. The WD 1236−495, used as a spectrophotometric standard (LTT 4816), has been discovered recently to be a ZZ Ceti variable, with a dominant period of ~600 s and an amplitude of about 0.004 mag (Kanaan et al. 1992). From our 10 spectra we obtain an average of $T_{\rm eff} \simeq 12{,}900$ K and a very high surface gravity of log $g = 8.7$ which corresponds to a mass of $1.02\ M_\odot$. From the results of an unpublished analysis by one of us (P. B.), LTT 4816 turns out to be the most massive ZZ Ceti star yet discovered, more massive than the second most massive one known (G207−9) by more than $0.25\ M_\odot$.

6. The WD 1422+095 is also a well known ZZ Ceti variable (GD 165; Bergeron et al. 1993), with a well separated companion (Zuckermann & Becklin 1987).

7. The WD 0612+177 (G104−27) is a DAB star in which Holberg, Kidder, & Wesemael (1990) have clearly identified the He I λ4471 and λ5015 features. At the lower spectral resolution of our observations, however, these features could not be detected.

6.2. *The Two WD+RD Pairs*

Two binary systems composed of a WD and a Red dwarf have been observed: 0034−211 and 0419−487. BGRD included them in their survey without being aware of the presence of a red dwarf companion (Probst & O'Connell 1982; Probst 1983). For statistical purposes one can consider them as independent spectroscopic rediscoveries of their binary nature.

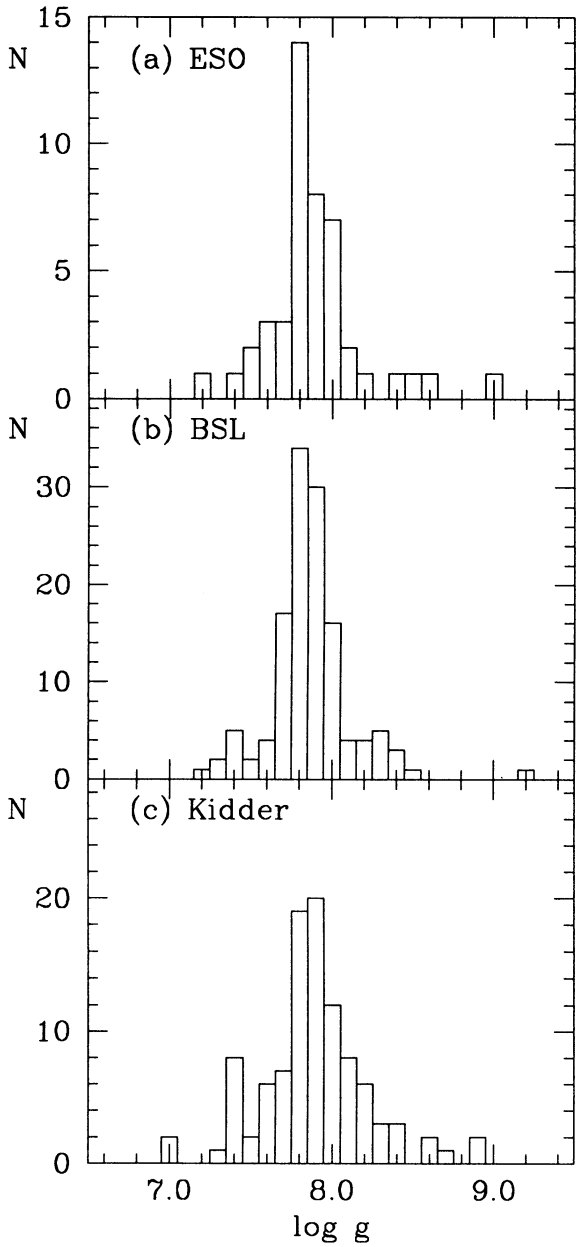

FIG. 10.—Gravity distributions (bin = 0.1 in log g) for the (*a*) ESO, (*b*) BSL, and (*c*) Kidder (1991) samples.

From their IR excess Probst (1983) estimated the companion of 0034−211 to be a ~dM4 star of nearly equal V-magnitude, and that of 0419−487 a fainter ($V \sim 14.7$) RD. The components of both binary systems are spatially unresolved. Spectra for the two objects covering the 3800–5300 Å interval are presented in Figure 3*d*. They have been obtained through the Blue150 grism at the ESO 3.6 m telescope; no flux calibration has been applied and the scale is arbitrary.

The object 0419−487 shows fairly large radial velocity changes in both the WD Balmer lines and the TiO bands of the RD, and there is a modest Hα emission. The system shows eclipses, has a photometric period of 7.3 hours (Krzeminski 1984) and may be a post common envelope-phase binary. BGRD obtained, from radial velocity measurements, a different period (12.9 hours), almost twice the photometric one. Since only 15 spectra were available for the analysis, and given the fairly large errors on those measurements and the relatively few data points, the radial velocity curve is not well defined, and we consider the photometric period to be more reliable. This is nevertheless a photometric *and* a double lined spectroscopic binary, and all the binary parameters could be derived. The system deserves further study.

In the WD 0034−211 system, all Balmer lines show an emission core, very strong in Hα, which is filled by the light of the RD companion responsible for the prominent TiO bands redwards of ~5000 Å. Instead of Roche-lobe overflow, BGRD considered that the Balmer emission is more likely caused by the fairly hot WD illuminating the RD companion, or by a wind from the WD which may help extracting material from the RD. No detectable changes in radial velocity or line profile have been noticed yet for this system.

As can be seen in Figure 3*d*, light contamination from the redder companion is fairly significant, even at short wavelengths. The light contamination from the red companion dilutes the line profiles from the white dwarf significantly, and models fits to these lines yield unreliable results. This problem is more critical for 0419−487 since the white dwarf component of the system has a low temperature (~7000 K), and its luminosity becomes comparable to that of the RD component, even at very short wavelengths. The situation is less problematic for 0034−311 because of the higher temperature of the WD component, although Hβ is still heavily contaminated. The adopted values are shown in Table 4 and have been obtained retaining all four values for 0034−211 and only the 18 more acceptable fits (of the 28 available spectra) for 0419−487. Notice that the higher temperature of 0034−211 may be responsible for the stronger Balmer line emission in this object.

7. DISCUSSION

7.1. *The Lower Mass Cutoff*

Current stellar evolution theory predicts a very precise low-mass cutoff for the WD mass distribution, resulting from the oldest stars (~15 Gyr) with an initial mass of ~0.85–0.9 $M_\odot$ leaving ~0.55 ± 0.01 $M_\odot$ WD remnants (Renzini & Fusi Pecci 1988; see also Figure 2 in Greggio & Renzini 1990, hereafter GR). Since the observed distribution peaks between 0.50 and 0.55 $M_\odot$ it appears that a small (but non-negligible) systematic error of ~0.05 $M_\odot$ is involved, that could be due to evolutionary theory, WD models, or model atmospheres. Each of these three options is now briefly discussed.

TABLE 4

WHITE DWARF PARAMETERS FOR THE TWO WD + RD PAIRS

Object	Name	V	n	$T_{\rm eff}$ (K)	$\sigma_{T_{\rm eff}}$	log g	$\sigma_{\log g}$	$M/M_\odot$	σ_M	M_V
0034−211.....	G266−141	14.53	4	17217	496	8.039	0.092	0.617	0.053	11.26
0419−487.....	LFT 349	14.36	18	7005	140	7.723	0.191	0.431	0.089	12.54

The lowest mass, single WDs in our sample are likely to be the remnants of the oldest stars in the Galactic disk, i.e., of stars at most ~ 15 Gyr old, and therefore with initial mass $M_i \gtrsim 0.85\ M_\odot$. As detailed in GR, the corresponding final mass is given by the core mass at the core helium flash (which takes place at the tip of the red giant branch), increased by the mass processed by the hydrogen burning shell during the subsequent evolutionary phases: the horizontal branch (HB), the early asymptotic giant branch (E-AGB), and the thermally pulsing AGB (TP-AGB), following the nomenclature introduced by Iben & Renzini (1983). Cumulatively, this amounts to an increase of $\sim 0.05\ M_\odot$ over the core mass at helium ignition, only slightly dependent on mass and composition. An inspection to GR Figures 2, 4, and 5 reveals that for solar metallicity ($\log Z = -1.7$) and an age of 15 Gyr the core mass at the first thermal pulse on the AGB is already $\sim 0.55\ M_\odot$, fairly insensitive to metallicity.

Globular cluster color-magnitude diagrams, coupled with the number of stars in each phase, provide a stringent check for the various steps above, i.e., for the core mass at the helium flash, as well as for the amount of fuel that is burned in the course of the HB and post-HB phases—and therefore of the corresponding increments of the core mass which take place during them. A reduction of $0.05\ M_\odot$ in the core at the helium flash would cause a reduction of ~ 0.4 mag in the HB luminosity, (see eq. [3.1] in Renzini 1977). This is at variance with the good agreement existing between theoretical and empirical HB luminosities (Renzini & Fusi Pecci 1988). It would also cause an *increase* of $\sim 40\%$ in the estimated age of globular clusters when using certain dating methods (Renzini 1991), bringing the age of the universe above ~ 20 Gyr, certainly not a popular value. In any event, the accuracy with which current evolutionary models are able to predict the core mass at the helium flash is believed to be very good, better than $\sim 0.01\ M_\odot$ (Sweigart 1994), and we conclude that an overestimate by $\sim 0.05\ M_\odot$ is unlikely to be the cause of the discrepancy.

Alternatively, one may appeal to a reduction in the fuel consumption during the HB and the E-AGB phases. According to standard models, the HB and E-AGB together contribute $\sim 25\%$ of the total light of an old stellar population. Again, this is in excellent agreement with what is empirically determined for globular clusters (Renzini & Fusi Pecci 1988). On the other hand, a fuel consumption of $0.05\ M_\odot$ of hydrogen corresponds to $\sim 10\%$ of the total light of an old population (see GR), and a reduction of this size in the HB + AGB fuel consumption would cause a drop of the combined contribution of these two phases from $\sim 25\%$ to $\sim 15\%$, thus destroying the good agreement with the observations. As extensively discussed in GR, a strong reduction in the amount of hydrogen processed during the HB and subsequent phases could be accomplished by invoking higher mass-loss rates during the RGB phase, thus producing hot HB stars and their AGB-manqué progeny. In such stars the thin hydrogen envelope is more likely lost in a wind rather than burned and incorporated into the degenerate core. WDs with masses as low as $\sim 0.5\ M_\odot$ could then be produced in this way. However, for this explanation to work, one would need a majority of helium burning

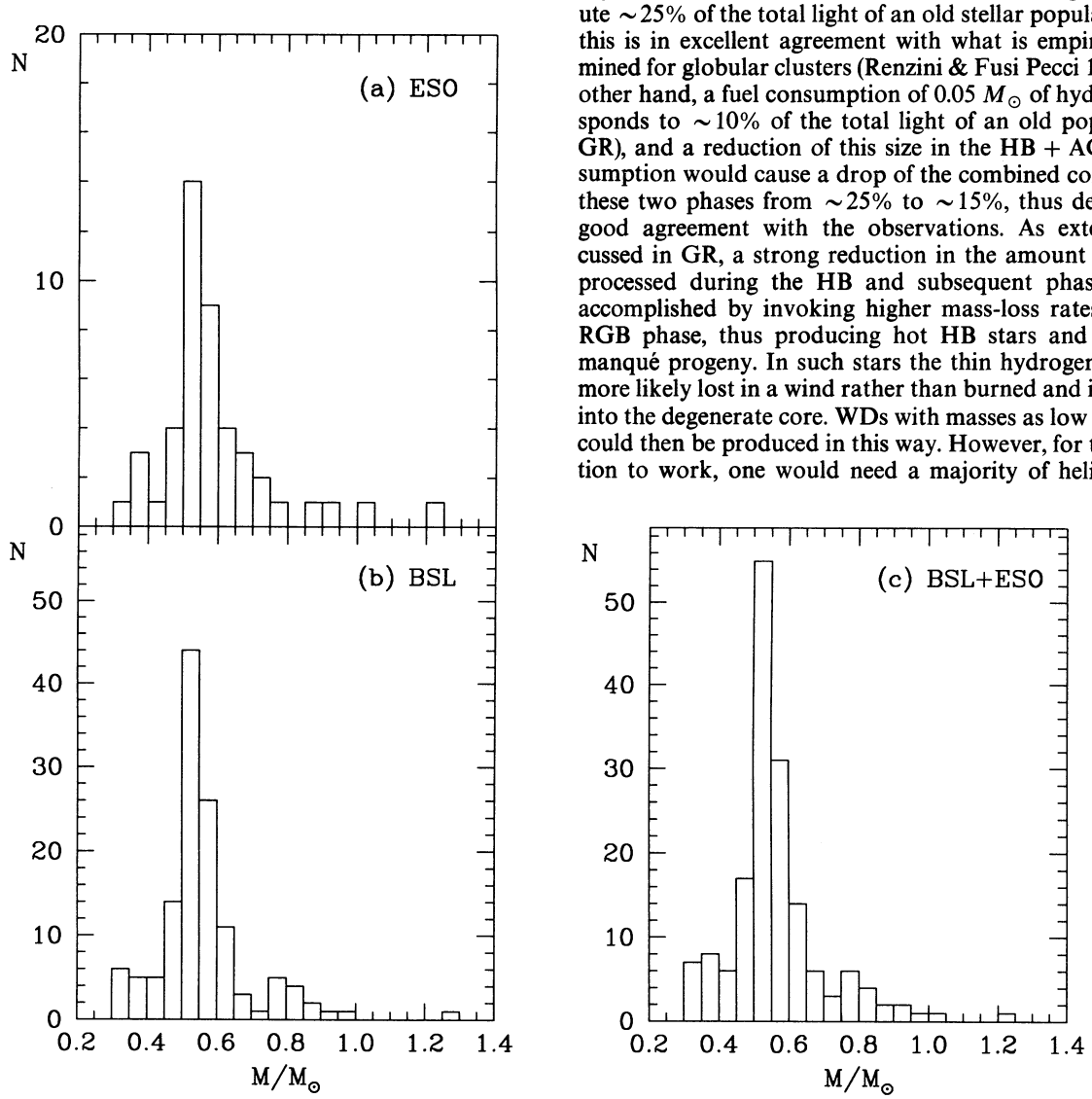

FIG. 11.—Mass distribution (bin = $0.05\ M_\odot$) for the 46 "hot" DA WDs in the ESO sample (*a*), the 129 in BSL (*b*), and the cumulative WD mass distribution for the 164 WDs in the combined sample (*c*).

phase stars in the solar neighborhood to belong to a hot HB and AGB-manqué sequence, i.e., spectroscopically looking as sdB, sdO, or low-mass WN stars (Heber 1992; GR). Stars of this kind are instead very rare in the solar vicinity as well as throughout the whole Galaxy, and is estimated that only $\lesssim 2\%$ of RGB stars lose enough mass to become hot subdwarfs (Heber 1986). We conclude that the theoretically estimated minimum mass of single WDs is unlikely to be appreciably lower than 0.55 $M_\odot$.

One may argue that the WD descendents of the oldest disk stars may not be as old as Galactic globular clusters, or may be metal-poor compared to the sun. However, assuming a lower age for the oldest WDs in our sample would go in the wrong direction, i.e., it would increase the core mass at the first thermal pulse, as a result of a more powerful hydrogen burning shell during the HB phase. The subsequent TP-AGB phase is most likely very short in low-mass, old stars, and in any event younger precursors being more massive, the core growth during the TP-AGB phase would be even larger, thus leading to larger final masses.

As a test of the spectroscopic method to determine masses, BSL have compared white dwarf masses derived from spectroscopy with those obtained from gravitational redshift measurements. The mean masses of both subsamples agree within $\sim 0.005\ M_\odot$. It is therefore unlikely that an underestimate as large as 0.05 $M_\odot$ may originate from systematic errors in the model spectrum calculations.

As noted before, empirical gravities have been translated to WD masses using the WD models of Wood (1990), and these models have been constructed assuming a pure carbon core, a very thin helium layer on top of it, and no hydrogen envelope at all. Actually, WDs are expected to be at least 50% oxygen, the mass of the helium layer is most likely two orders of magnitude larger than adopted by Wood (Iben & McDonald 1986; Koester & Shönberner 1986), and DAs certainly have a hydrogen envelope, which in a typical 0.6 $M_\odot$ WD may be as thick as $10^{-4}\ M_\odot$ (Iben & Tutukov 1985). The effects of these three parameters on the derived spectroscopic masses have been estimated by BSL. The first two effects have been shown to be completely negligible ($\sim 0.004\ M_\odot$). On the other hand, BSL estimated that spectroscopic masses could be appreciably underestimated if white dwarf stars had thick hydrogen layers, by as much as $\sim 0.04\ M_\odot$ for a 0.6 $M_\odot$ WD with a $10^{-4}\ M_\odot$ hydrogen rich envelope. The case is illustrated in Figure 12.

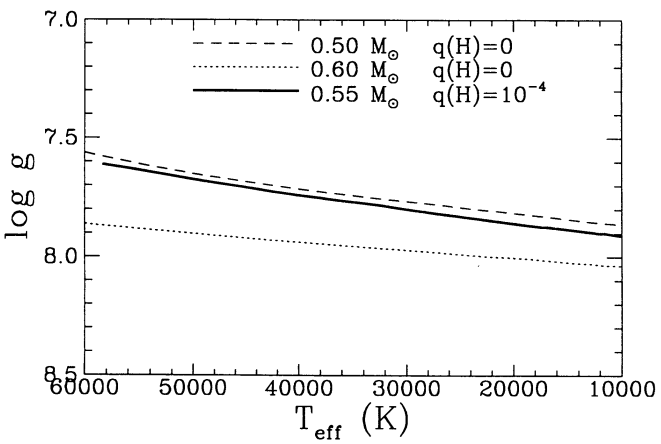

FIG. 12.—Effects of changing hydrogen layer mass on stellar models shown in the $T_{\rm eff}$-log g plane (see text).

The effect appears to be somewhat less pronounced in the models of Koester & Schönberner (1986). BSL concluded that the use of the evolutionary models of Wood (1990) with no hydrogen layer was justified after all, as apparently compelling arguments were favoring extremely thin hydrogen envelopes (see, e.g., Fontaine & Wesemael 1987). However, our understanding of the envelope structure of WD stars has changed substantially in the last few years, and we briefly discuss some of the most important results.

Arguments favoring a very thin hydrogen envelope were first presented by Winget & Fontaine (1982), who investigated the sensitivity of the pulsation properties of ZZ Ceti stars to the mass of the hydrogen envelope, and concluded that the observed blue edge of the ZZ Ceti instability strip could only be reproduced by models with very thin hydrogen envelopes ($< 10^{-8}\ M_\odot$). However, recent, more accurate non-adiabatic calculations now show that the blue edge temperature of the ZZ Ceti instability strip is actually insensitive to the mass of the hydrogen envelope (Fontaine et al. 1994; Bradley & Winget 1994), and therefore cannot set constraints on it.

Independent evidence for thin hydrogen envelope came also from the analysis of Vennes et al. (1988), who argued that the EUV/X-ray flux deficiency observed in hot DA WDs could only be accounted for assuming an extremely thin hydrogen envelope (10^{-14}–$10^{-13}\ M_\odot$), provided helium being the main source of opacity. However, Vennes et al. (1989) demonstrated that in at least one star (Feige 24) the missing source of opacity comes instead from a host of heavy elements supported by radiative acceleration. More recently, Barstow et al. (1993) have shown from *ROSAT* observations that trace elements heavier than helium are likely to provide most of the missing opacity in DA stars hotter than 40,000 K. Consequently, thin hydrogen layers are no longer required to explain the EUV/X-ray flux deficiency. In the same context, Vennes et al. (1988) argued that stratified atmospheres with thin hydrogen layers were the only viable explanation to account for the presence of helium in the spectra of DAO stars (He II λ4686). However, the spectroscopic analysis of a larger sample of DAO stars by Bergeron et al. (1994) has convincingly demonstrated that the optical spectra of DAO stars are better reproduced by models with *homogeneous* atmospheres while stratified atmospheres with extremely thin hydrogen layers do not reproduce the observations.

Fontaine & Wesemael (1987) suggested that perhaps the majority of all WDs may have evolved from helium-rich PG 1159 stars. As these stars cool down, any trace residual hydrogen in the helium-rich envelope would eventually diffuse upward, and an optically thick hydrogen atmosphere would be gradually built up, transforming a helium-rich atmosphere into a hydrogen-rich atmosphere, i.e., a non-DA into a DA WD. Such DA WDs would retain thin hydrogen layers throughout their evolution. However, there has been increasing acceptance to the empirical notion that the hydrogen-poor/hydrogen-rich dichotomy pre-exists the WD stage, being already present among planetary nebula nuclei (Smith & Aller 1969; Heap 1982; Mendez et al. 1986; Napiwotzki & Schönberner 1993), with the majority of objects being hydrogen rich. Thus, most WDs enters directly the DA evolutionary channel with a hydrogen-rich composition, and there is no need to appeal to very thin hydrogen atmospheres as it was required in the frame of the Fontaine & Wesemael scenario. We recall that the hydrogen-poor/hydrogen-rich dichotomy among planetary nebula nuclei and WDs as well is most naturally explained as a

result of some Post-AGB stars experiencing a final helium shell flash (Renzini 1979, 1982), a scenario for which there is now more compelling observational evidence including the real time metamorphoses of Post-AGB stars into hydrogen-poor objects such as R CrB stars (Bond, Liebert, & Renzini 1992; Jurcsik 1993; Iijima & Strafella 1994) and WN planetary nebula nuclei (Peña et al. 1994).

Even though thin hydrogen layers may still be required to explain the observed deficiency of helium-rich white dwarfs between 45,000 and 30,000 K (the so-called DB gap), the hydrogen layer mass in DA stars is less constrained than previously believed. Hence, it is entirely plausible that most DA stars have hydrogen layers as massive as indicated by evolutionary models, in which case for $M \lesssim 0.6\ M_\odot$ spectroscopic masses would increase by $\sim 0.04\ M_\odot$, thus resolving the above mentioned discrepancy between the observed mass distribution of WDs and that expected from stellar evolution theory. We note however that all available WD models have been computed with what are now called the *old* opacities. The *new* radiative opacities (Rogers & Iglesias 1992) are significantly higher than the old ones at intermediate temperatures, when most of the absorption is due to highly ionized metals. An increase in the opacity is expected to lead to a larger radius, lower gravity and lower inferred mass, for WDs of given luminosity. The size of the effect remains however to be determined. Apart from this surviving uncertainty, all other evidences now suggest that WD models with evolutionary (i.e., thick) envelope masses should be used in translating gravities into WD masses, and we intend to do so in the future for the whole sample of available WDs.

7.2. *The Initial Mass to Final Mass Relation*

It has been known since a long time that mass loss on the AGB can effectively strip most of the hydrogen envelope and leave WD remnants for stars with $M_i = 4$–$8\ M_\odot$, when using either a theoretically motivated, solar-scaled rate of mass loss (Fusi Pecci & Renzini 1975), or an empirical mass-loss rate (such as that introduced by Reimers 1975), when conveniently parameterized with the so called η parameter (Fusi Pecci & Renzini 1976). An analytical expression for the corresponding IMFMR (hereafter the *old* IMFMR) is given by Iben & Renzini (1983; see also Renzini & Voli 1981). It was soon realized that this old IMFMR leads to WD mass distributions that are definitely broader than the observed one when coupled with reasonable galactic histories of star formation (Koester & Weidemann 1980), with a sizable excess of objects more massive than $\sim 0.7\ M_\odot$.

Parallel to these findings, it was realized that the same synthetic AGB models producing the old IMFMR, also predicted a population of bright AGB stars for which there was but a very scanty evidence in extensive surveys of the Magellanic Clouds (see Iben & Renzini 1983, and references therein). Clearly, synthetic AGB models were generating an excessive number of massive core (then bright) AGB stars, which in turn were leaving too many massive WDs. This major discrepancy—sometimes referred to as the "AGB mystery"—has polarized the attention for the following decade.

To solve the problem, enhanced mass loss on the AGB—in excess of the standard parameterization—has been most widely invoked, and a variety of alternative parameterizations have been proposed (for a recent review see Weidemann 1993). Actually, the inadequacy of the old IMFMR stems from two erroneous assumptions in Renzini & Voli (1981), which can be traced back to Fusi Pecci & Renzini (1976) and Iben & Truran (1978): (1) a too steep dependence of the core mass at the beginning of the TP-AGB phase as a function of mass for $M_i \lesssim 3\ M_\odot$, and (2) the use of a unique core mass-luminosity relation on the AGB.

Concerning the first point, for the lack of suitable models in the literature, Iben and Truran (and Renzini and Voli following them) were forced to interpolate linearly between a $0.6\ M_\odot$ model and a $3\ M_\odot$ model, thus overlooking the nonmonotonic behavior of several evolutionary quantities in this mass range, a result of the sharp transition around $\sim 2\ M_\odot$ between stars which develop a degenerate helium core on the RGB and those which do not (e.g., Sweigart, Greggio, & Renzini 1990). In reality, for $1 \lesssim M_i \lesssim 3\ M_\odot$ the core mass at the first pulse runs much flatter as a function of M_i than resulting from the old interpolation (Lattanzio 1987, 1989), which results in a seemingly flatter $M_f(M_i)$ relation, and therefore in a more peaked WD mass distribution.

The inadequacy of the assumption of a universal core mass-luminosity relation was not discovered until recently. Indeed, Blöcker & Schönberner (1991) have constructed evolutionary TP-AGB models for a $7\ M_\odot$ star, having adopted a mixing-length parameter $\alpha = 2$. As expected for this combination of mass and α (Renzini & Voli 1981), their TP-AGB models experience a strong *envelope burning* process (i.e., the convective envelope reaches well into the hydrogen burning shell). But, most surprisingly, the luminosity evolution is much faster than predicted by the classical core mass-luminosity relation (Paczyński 1970). This result has been also confirmed in independent calculations by Boothroyd & Sackmann (1992) and Lattanzio (1992), and we can take for established that for stars experiencing the envelope burning process the stellar luminosity is a complicated, yet to be fully explored function not only of core mass, but also of total mass, mixing-length parameter α, and composition. These calculations suggest that, climbing quickly to very high luminosity, the more massive AGB star models which experience envelope burning may run into severe mass loss even when using a conservative mass-loss rate, thus leaving the AGB and evolving towards their final WD configuration. The rapid luminosity increase may also anticipate the transition to the so-called *superwind* regime, that is needed to produce the observed planetary nebulae (Renzini 1981). The net result of all this is a reduction of the TP-AGB lifetime and of the amount of fuel that is burned during this phase, thus reducing considerably the mass of the WD remnant over the value predicted by the standard core mass luminosity relation. However, the exploration of this very attractive possibility of solving the long standing dilemma requires extensive calculations yet to be made, as those so far available in the literature appear to be insufficient to generate a reasonably well founded theoretical IMFMR (Greggio & Renzini 1995).

Notwithstanding these complications, we recall that the envelope burning process sets in very sharply above a threshold value of the core mass ($\sim 0.9\ M_\odot$) and of the total mass, the latter between ~ 3.3 and $4\ M_\odot$, for $1.5 \lesssim \alpha \lesssim 2$ (Renzini & Voli 1981), i.e., for values of α in the most plausible range. It is therefore quite possible that even the most massive AGB stars ($M_i \simeq 9\ M_\odot$) may soon lose their entire hydrogen-rich envelope, with thus only very modest increase of the core mass over its value at the beginning of the TP-AGB phase ($\sim 1.06\ M_\odot$ for $M_i = 9\ M_\odot$). This would imply a maximum mass for C-O WDs very close to $\sim 1.1\ M_\odot$ (well below the

Chandrasekhar limit!), in excellent agreement with the maximum mass of the observed distribution (see Fig. 11). Empirical evidence that stars as massive as $\sim 8\ M_\odot$ may leave WD remnants also come from WDs that are members of young open clusters (Romanishin & Angel 1980; Weidemann 1993, and references therein).

Thus, on the theoretical point of view the maximum mass of single-born WDs turns out to be a function of the efficiency of the envelope burning process and therefore of the mixing-length parameter α. Several pertinent calibrations of α can be envisaged. A first possibility is offered by the AGB luminosity function of Magellanic Cloud fields and clusters. Clearly, the finding that with envelope burning process the TP-AGB lifetime is shortened—selectively for the most massive and brightest AGB stars—offers a most natural solution to the AGB mystery (Renzini 1992). Again, by properly tuning α, a reasonably good fit with the observed AGB luminosity function may be reached. This automatically would also ensure a better agreement between calculated and observed WD mass distributions, by selectively reducing the predicted mass *only* for WDs more massive than $\sim 0.9\ M_\odot$, the minimum core mass for the envelope burning process to occur. This means that a virtually unique value of α—well within the range $1.5 \lesssim \alpha \lesssim 2$—may at once reproduce the solar radius, the location in the HR diagram of local subdwarfs and globular cluster red giants (see Fusi Pecci & Renzini 1988, and references therein), as well as the luminosity function of AGB stars in the Magellanic Clouds and the WD mass distribution in the solar neighborhood.

But what independent evidence there exists for the envelope burning process being really active in massive AGB stars? Fairly direct evidence comes from the high, super-cosmic lithium abundance that is observed in bright AGB stars of the Magellanic Clouds (Smith & Lambert 1989; Plez, Smith, & Lambert 1993). Indeed, with the temperature at the base of the convective envelope reaching values in excess of $\sim 4 \times 10^7$ K, the ^{3}He synthetized during the main sequence phase is rapidly processed to ^{7}Li in the brightest AGB stars (Sackmann, Smith, & Despain 1974; Iben 1975; Renzini 1983) via the mechanism first envisaged by Cameron & Fowler (1971). Detailed calculations of the lithium enrichment in AGB star envelopes have been recently presented by Sackmann & Boothroyd (1992). Another signature of the envelope burning process is represented by the very low $^{12}C/^{13}C$ ratio exhibited by part of the pristine interstellar grains included in primitive meteorites (Anders & Zinner 1993), and we conclude that solid empirical evidence actually exists for the envelope burning process being indeed active in brightest AGB stars. Thus, it seems to us that the Blöcker and Schönberner discovery of the breakdown of the core mass-luminosity relation offers a very attractive possibility of accounting for both the luminosity function of AGB stars in the Magellanic Clouds and the WD mass distribution in the solar neighborhood, thus superseding all previous attempts to cope with the AGB mystery (a fairly extended list of them being mentioned by Weidemann 1993).

The resulting IMFMR, starting at $M_f \simeq 0.55\ M_\odot$ for $M_i \simeq 1\ M_\odot$, running much flatter than the old one below $M_i \simeq 2.5\ M_\odot$, and terminating at $M_f \simeq 1.1\ M_\odot$ for $M_i = 9\ M_\odot$, will also be in excellent agreement with the semi-empirical IMFMR advocated by Weidemann (1987) on the basis of the masses of WD members of Galactic open clusters. However, as mentioned above, an attempt at putting into more quantitative terms these qualitative considerations requires extensive stellar evolutionary calculations for TP-AGB stars experiencing envelope burning, i.e., a major computational effort.

We finally comment again on the absence of gaps and secondary peaks in the mass distribution. Clearly, features in the IMFMR inprint features in the WD mass distributions: where the relation $M_f(M_i)$ runs flat many stars leave remnants with nearly the same mass and a peak is produced, while where $M_f(M_i)$ is steep few WDs in a certain mass interval are generated, thus resulting in a gap in the mass distribution. This is indeed the origin of the main, very prominent peak characterizing the mass distribution, that is due to the final mass varying very little for $M_i \lesssim 2.5\ M_\odot$. Thus, the absence of other prominent features argues for the IMFMR running rather smoothly for $M_i \gtrsim 2.5\ M_\odot$, i.e., without further large variations of slope. Errors are certainly not completely negligible, however, and they tend to wash out features in the mass distribution. For this reason, further improving both the accuracy of the mass determinations and the number of observed WDs would seem a worthwhile effort, especially increasing the statistics for WD masses in excess of $\sim 0.7\ M_\odot$.

A. B. acknowledges the support of the Consiglio Nazionale per le Ricerche for a fellowship and the hospitality of the Lunar and Planetary Laboratory (AZ). She also wishes to thank R. A. Saffer for this kind and expert introduction to spectroscopic data reductions with IRAF and J. Holberg, K. Kidder, and R. A. Saffer for many helpful discussions. This work was supported in part by the NSERC Canada, and by the Fund FCAR (Québec). A. R. acknowledges the hospitality of ESO, where part of a first draft of this paper was written. We are also indebted with H. Ritter for references on previous, unnoticed work on WD 0419−487. Finally we wish to thank the anonymous referee whose skilful comments helped much in improving the manuscript quality. This research has made use of the SIMBAD database, operated at CDS, Strasbourg, France.

REFERENCES

Anders, E., & Zinner, E. 1993, Meteoritics, 28, 490
Barstow, M. A., et al. 1993, MNRAS, 264, 16
Bergeron, P. 1993, in White Dwarfs: Advances in Observation and Theory, NATO ASI Series, ed. M. A. Barstow (Dordrecht: Kluwer), 267
Bergeron, P., Fontaine, G., Brassard, P., Lamontagne, R., & Wesemael, F. 1993, AJ, 106, 1987
Bergeron, P., Kidder, K., Holberg, J., Liebert, J., Wesemael, F., & Saffer, R. A. 1991, ApJ, 372, 267
Bergeron, P., Saffer, R. A., & Liebert, J. 1992, ApJ, 394, 228 (BSL)
Bergeron, P., Wesemael, F., Beauchamp, A., Wood, M. A., Lamontagne, R., Fontaine, G., & Liebert, J. 1994, ApJ, 432, 305
Bergeron, P., Wesemael, F., & Fontaine, G. 1991, ApJ, 367, 253
———. 1992, ApJ, 387, 288
Bergeron, P., Wesemael, F., Fontaine, G., & Liebert, J. 1990, ApJ, 351, L21
Bergeron, P., Wesemael, F., Lamontagne, R., Fontaine, G., Allard, N. F., & Saffer, R. A. 1995b, in preparation
Bergeron, P., Wesemael, F., Liebert, J., & Fontaine, G. 1989, ApJ, 345, L91
Blöcker, T., & Schönberner, D. 1991, A&A, 244, L43
Bond, H. E., Liebert, J., & Renzini, A. 1992, in Science with the *Hubble Space Telescope*, ed. P. Benvenuti & Q. E. Schreier (Garching: ESO), 139
Boothroyd, A. I., & Sackman, I.-J. 1992, ApJ, 393, L21
Bradley, P. A., & Winget, D. E. 1994, ApJ, 421, 236
Bragaglia, A., Greggio, L., & Renzini, A. 1995, in preparation
Bragaglia, A., Greggio, L., Renzini, A., & D'Odorico 1990, ApJ, 365, L13, (BGRD)
Cameron, A. G. W., & Fowler, W. A. 1971, ApJ, 164, 111
Fontaine, G., Brassard, P., Wesemael, F., & Tassoul, M. 1994, ApJ, 428, L61
Fontaine, G., & Wesemael, F. 1987, in IAU Colloq. 95, The Second Conference on Faint Blue Stars, ed. A. G. D. Philip, D. S. Hayes, & J. Liebert (Schenectady: Davis), 319
Fusi Pecci, F., & Renzini, A. 1975, Mem. Soc. R. Sci. Liège, 6th Ser., 6, 383
———. 1976, A&A, 46, 447

Green, R. F. 1980, ApJ, 238, 685
Greggio, L., & Renzini, A. 1990, ApJ, 364, 35 (GR)
———. 1995, in preparation
Guseinov, O. H., Novruzova, H. I., & Rustamov, Y. S. 1983, Ap&SS, 96, 1
Hamada, T., & Salpeter, E. E. 1961, ApJ, 134, 683
Heap, S. R. 1982, in Wolf-Rayet Stars: Observation, Physics, Evolution, ed. C. W. H. de Loore & A. J. Willis (Dordrecht: Reidel), 423
Heber, U. 1986, A&A, 155, 33
———. 1992, in The Atmospheres of Early-Type Stars, ed. U. Heber & C. S. Jeffery (Berlin: Springer), 233
Holberg, J. B., Kidder, K. M., & Wesemael, F. 1990, ApJ, 365, L77
Iben, I., Jr. 1975, ApJ, 196, 525
Iben, I., Jr., & Laughlin, G. 1989, ApJ, 341, 312
Iben, I., Jr., & MacDonald, J. 1986, ApJ, 301, 164
Iben, I., Jr., & Renzini, A. 1983, ARA&A, 21, 271
Iben, I., Jr., & Truran, J. W. 1978, ApJ, 220, 980
Iben, I., Jr., & Tutukov, A. V. 1984, ApJS, 54, 335
———. 1985, ApJS, 58, 661
———. 1986, ApJ, 311, 742
Iijima, T., & Strafella, F. 1994, Inf. Bull. Var. Stars, No 3959
Jurcsik, J. 1993, Acta Astron., 43, 353
Kanaan, A., Kepler, S. O., Giovannini, O., & Diaz, M. 1992, ApJ, 390, L89
Kidder, K. 1991, Ph.D. thesis, Univ. Arizona
Koester, D., & Schönberner, D. 1986, A&A, 154, 125
Koester, D., Schulz, H., & Weidemann, V. 1979, A&A, 76, 262 (KSW)
Koester, D., & Weidemann, V. 1980, A&A, 81, 45
Krzeminski, W. 1984, IAU Circ. 4014
Lattanzio, J. 1987, ApJ, 313, L15
———. 1989, in Evolution of Peculiar Red Giant Stars, ed. H. Johnson & B. Zuckerman (Cambridge: Cambridge Univ. Press), 161
———. 1992, private communication
McCook, G. P., & Sion, E. M. 1987, ApJS, 65, 603
McMahan, R. K. 1989, ApJ, 336, 409
Mendez, R. H., Miguel, C. H., Heber, U., & Kudritzki, R. P. 1986, in Hydrogen Deficient Stars and Related Objects, ed. K. Hunger et al. (Dordrecht: Reidel), 323
Napiwotzki, R., & Schönberner, D. 1993, in White Dwarfs: Advances in Observation and Theory, ed. M. A. Barstow (Dordrecht: Kluwer), 99
Paczyński, B. 1970, Acta Astron., 20, 1
———. 1985, in Cataclysmic Variables and Low-Mass X-ray Binaries, ed. D. Q. Lamb & J. Patterson (Dordrecht: Reidel), 1
Peña, M., Torres-Peimbert, S., Peimbert, M., Ruiz, M. T., & Maza, J. 1994, ApJ, 428, L9
Plez, B., Smith, V. V., & Lambert, D. L. 1993, ApJ, 418, 812
Pounds, K. A., et al. 1993, MNRAS, 260, 77
Probst, R. G. 1983, ApJS, 53, 335
Probst, R. G., & O'Connell, R. W. 1982, ApJ, 259, L69
Reimers, D. 1975, Mem. Soc. R. Sci. Liège, 6th Ser., 6, 369
Renzini, A. 1977, in Advanced Stages in Stellar Evolution, ed. P. Bouvie & A. Maeder (Geneva: Geneva Obs.), 149
Renzini, A. 1979, in Stars and Star Systems, ed. B. E. Westerlund (Dordrecht: Reidel), 155
———. 1981, in Physical Processes in Red Giants, ed. I. Iben, Jr. & A Renzini (Dordrecht: Reidel), 431
———. 1982, in Wolf-Rayet Stars: Observation, Physics, Evolution, ed. C. W. H. de Loore & A J. Willis (Dordrecht: Reidel), 423
———. 1983, in Primordial Helium, ed. P. A. Shaver et al. (Garching: ESO), 109
———. 1991, in Observational tests of Cosmological Inflation, ed. T. Shanks et al. (Dordrecht: Kluwer), 131
———. 1992, in The Stellar Populations of Galaxies, ed. B. Barbuy & A. Renzini (Dordrecht: Kluwer), 325
———. 1993, in Supernovae and Supernova Remnants, ed. R. McCray (Cambridge: Cambridge Univ. Press), in press
Renzini, A., & Buzzoni, R. 1986, in Spectral Evolution of Galaxies, ed. C. Chiosi & A. Renzini (Dordrecht: Reidel), 135
Renzini, A., & Fusi Pecci, F. 1988, ARA&A, 26, 199
Renzini, A., & Voli, M. 1981, A&A, 94, 175
Rogers, F. J., & Iglesias, C. A. 1992, ApJS, 79, 507
Romanshin, W., & Angel, J. R. P. 1980, ApJ, 235, 992
Sackmann, I. J., & Boothroyd, A. I. 1992, ApJ, 392, L71
Sackmann, I.-J., Smith, R. L., & Despain, K. H. 1974, ApJ, 187, 555
Saffer, R. A., Liebert, J., & Olszewski, E. W. 1988, ApJ, 334, 947
Shipman, H. L. 1979, ApJ, 228, 240
Smith, L. F., & Aller, L. H. 1969, ApJ, 157, 1245
Smith, V. V., & Lambert, D. L. 1989, ApJ, 345, L75
Sweigart, A. V. 1994, ApJ, 426, 612
Sweigart, A. V., Greggio, L., & Renzini, A. 1990, ApJ, 364, 527
Taylor, J. R. 1982, An Introduction to Error Analysis (Mill Valley: University Science)
Vennes, S., Chayer, P., Fontaine, G., & Wesemael, F. 1989, ApJ, 336, L25
Vennes, S., Pelletier, C., Fontaine, G., & Wesemael, F. 1988, ApJ, 331, 876
Webbink, R. F. 1984, ApJ, 277, 355
Weidemann, V. 1987, A&A, 188, 74
———. 1990, ARA&A, 28, 105
———. 1993, in Mass Loss on the AGB and Beyond, ed. H. Schwarz (Garching: ESO), 55
Weidemann, V., & Koester, D. 1984, A&A, 132, 195
Wesemael, F. 1980, ApJS, 45, 177
Winget, D. E., & Fontaine, G. 1982, in Pulsations in Classical and Cataclysmic Variable Stars, ed. J. P. Cox & C. J. Hansen (Boulder: University of Colorado), 46
Winget, D. E., Hansen, C. J., Van Horn, H. M., Fontaine, G., Nather, R. E., Kepler, S. O., & Lamb, D. Q. 1987, ApJ, 315, L77
Wood, M. A. 1990, Ph.D. thesis, Univ. Texas at Austin
———. 1992, ApJ, 386, 539
Yungelson, L. R., Livio, M., Tutukov, A. V., & Saffer, R. A. 1994, ApJ, 420, 336
Zuckermann, B., & Becklin, E. D. 1987, ApJ, 319, L99